Single axon IPSPs elicited in pyramidal cells by three classes of interneurones in slices of rat neocortex

Alex M. Thomson, David C. West*, Joel Hahn and Jim Deuchars

*Royal Free Hospital School of Medicine, Rowland Hill Street, London NW3 2PF and *Department of Visual Sciences, Institute of Ophthalmology, Bath Street, London EC1V 9EL, UK*

1. Using dual intracellular recordings in slices of adult rat neocortex, twenty-four IPSPs activated by single presynaptic interneurones were studied in simultaneously recorded pyramidal cells. Fast spiking interneurones inhibited one in four or five of their close pyramidal neighbours. No reciprocal connections were observed. After recordings neurones were filled with biocytin.

2. Interneurones that elicited IPSPs were classified as classical fast spiking ($n = 10$), as non-classical fast spiking ($n = 3$, including one burst-firing interneurone), as unclassified, or slow interneurones ($n = 8$), or as regular spiking interneurones ($n = 3$), i.e. interneurones whose electrophysiological characteristics were indistinguishable from those of pyramidal cells.

3. All of the seven classical fast spiking cells anatomically fully recovered had aspiny, beaded dendrites. Their partially myelinated axons ramified extensively, varying widely in shape and extent, but randomly selected labelled axon terminals typically innervated somata and large calibre dendrites on electron microscopic examination. One 'autapse' was demonstrated. One presumptive regular spiking interneurone axon made four somatic and five dendritic connections with unlabelled targets.

4. Full anatomical reconstructions of labelled classical fast spiking interneurones and their postsynaptic pyramids ($n = 5$) demonstrated one to five boutons per connection. The two recorded IPSPs that were fully reconstructed morphologically (3 and 5 terminals) were, however, amongst the smallest recorded (< 0·4 mV). Some connections may therefore involve larger numbers of contacts.

5. Single axon IPSPs were between 0·2 and 3·5 mV in average amplitude at −55 to −60 mV. Extrapolated reversal potentials were between −70 and −82 mV. IPSP time course correlated with the type of presynaptic interneurone, but not with IPSP latency, amplitude, reversal potential, or sensitivity to current injected at the soma.

6. Classical fast spiking interneurones elicited the fastest IPSPs (width at half-amplitude 14·72 ± 3·83 ms, $n = 10$) and unclassified, or slow interneurones the slowest (56·29 ± 23·44 ms, $n = 8$). Regular spiking interneurone IPSPs had intermediate half-widths (27·3 ± 3·68 ms, $n = 3$).

7. Increasingly brief presynaptic interspike intervals increased the peak amplitude of, but not the area under, the summed IPSP. Only at interspike intervals between 10 and 20 ms did IPSP integrals exhibit paired pulse facilitation. Paired pulse depression was apparent at < 10 and 20–60 ms. During longer spike trains, summing IPSPs decayed to a plateau potential that was relatively independent of firing rate (100–250 Hz). Thereafter, the voltage response could increase again.

8. Summed IPSPs elicited by two to fifteen presynaptic spike trains decayed as, or more rapidly than, single-spike IPSPs. Summed IPSPs elicited by > 20 spikes (> 150 Hz), however, resulted in an additional, more slowly decaying component (latency > 50 ms, duration > 200 ms). The possible involvement of $GABA_B$ receptors in this component is discussed.

9. It is suggested that three broad classes of interneurones may activate $GABA_A$ receptors on relatively proximal portions of neocortical pyramidal neurones. The different time courses of the IPSPs elicited by the three classes may reflect different types of postsynaptic receptor rather than dendritic location. An additional class, burst firing, spiny interneurones appear to activate $GABA_A$ receptors on more distal sites.

Many different morphological classes of GABAergic (γ-aminobutyric acidergic) interneurones have been described in cortical regions. The axons of some of these have been shown to target very specifically certain regions of postsynaptic principle cells (e.g. Han, Buhl, Lörinczi & Somogyi, 1993). For example, chandelier (or axo-axonic) cells innervate predominantly the axon initial segments (Somogyi, 1977; Gulyás, Toth, Danos & Freund, 1991; Li, Somogyi, Tepper & Buzsáki, 1992; Gulyás, Miles, Hájos & Freund, 1993; Buhl, Han, Lörinczi, Stezhka, Karnup & Somogyi, 1994*b*; Del-Rio & DeFelipe, 1994; Condé, Lund, Jacobowitz, Baimbridge & Lewis, 1994), while basket cells innervate the somata and proximal dendrites of pyramidal cells (Jones & Hendry, 1984; Kisvárday, 1992; Kisvárday, Beaulieu & Eysel, 1993; Gulyás *et al.* 1993; Sik, Penttonen, Ylinen & Buzsáki, 1995). The majority of cells in these two classes are immunopositive for parvalbumin (Celio, 1986) and have smooth, aspiny dendrites. Smooth, parvalbumin-positive neocortical interneurones often display a classical fast spiking behaviour (Kawaguchi & Kubota, 1993). In the hippocampus and dentate gyrus, fast spiking basket and chandelier cells (Miles & Wong, 1984; Miles, 1990; Buhl, Halasy & Somogyi, 1994*a*; Buhl, Cobb, Halasy & Somogyi, 1995) activate fast IPSPs in a high proportion of simultaneously recorded principle neurones (Miles, 1990, 1991) and provide up to eight (chandelier) and twelve (basket) terminals to their postsynaptic targets (Buhl *et al.* 1994*a*). Single axon fast IPSPs are also capable of delaying postsynaptic action potentials and entraining the membrane potential oscillations and firing of postsynaptic CA1 pyramidal neurones (Miles & Wong, 1984; Miles, 1991; Cobb, Buhl, Halasy, Paulsen & Somogyi, 1995).

Another broad class of neocortical GABAergic interneurones display low threshold spiking (or burst-firing) behaviour, have sparsely to medium spiny dendrites and are calbindin immunoreactive (Kawaguchi & Hama, 1988; Kawaguchi & Kubota, 1993). The calbindin immunopositive axon terminals of double bouquet cells appear to innervate more distal regions of pyramidal dendritic trees than parvalbumin-positive terminals (DeFelipe, Hendry & Jones, 1989) and the fast IPSPs activated by spiny, burst-firing interneurones appear more readily recorded in postsynaptic pyramidal dendrites than in somata (Deuchars & Thomson, 1995*a*).

While basket and chandelier cells have been well described in both neocortex and hippocampus, it is less clear whether the parvalbumin-negative classes of interneurone in the two regions are direct equivalents of one another. However, hippocampal bistratified interneurones innervate both basal and apical dendrites of CA1 pyramidal cells (Buhl *et al.* 1994*a*) and one such cell has been shown to be calbindin-immunoreactive (Sik *et al.* 1995). In addition, bistratified interneurones display inherent electrophysiological characteristics that differ from those of basket cells. Bistratified neurones had higher input resistances, longer time constants, broader action potentials and shallower spike after-hyperpolarizations (AHPs) than basket cells (Buhl, Szilágyi, Halasy & Somogyi, 1996). In these properties they resembled the low threshold spiking cells in neocortex (Kawaguchi & Kubota, 1993; Deuchars & Thomson, 1995*a*, *b*; Thomson, West & Deuchars, 1995) and were distinguishable from basket cells even though basket cells did not display uniformly classical fast spiking activity or bistratified cells uniformly burst-firing behaviour. Hippocampal bistratified neurones have been shown to activate IPSPs in CA1 pyramids that are significantly slower in time course than those activated by basket or chandelier cells (Buhl *et al.* 1994*a*).

Several previous studies have therefore begun to correlate the properties of the GABAergic IPSPs with the physiological and morphological characteristics of the presynaptic interneurones in hippocampus and dentate gyrus. To date, only one such IPSP, generated by a spiny, burst-firing interneurone, has been reported in the neocortex and no direct information is available about the amplitude and time course of IPSPs activated by classical fast spiking interneurones in the neocortex. In addition to a potentially vast array of possible $GABA_A$ receptor subunit combinations (for reviews see Lüddens, Korpi & Seeburg, 1995; Sieghart, 1995), $GABA_B$ receptor-mediated IPSPs have been reported in many previous studies involving electrical stimulation in neocortical slices (e.g. Connors, Malenka & Silva, 1988). Several studies indicate that $GABA_A$ and $GABA_B$ receptors may be activated by different presynaptic interneurones in cortex (Sugita, Johnson & North, 1992; Benardo, 1994; Kang, Kaneko, Ohishi, Endo & Araki, 1994) and hippocampus (Lacaille & Schwartzkroin, 1988; Otis & Mody, 1992; Williams & Lacaille, 1992; Samulack & Lacaille, 1993). However, only a few hippocampal (e.g. Lacaille & Schwartzkroin, 1988) and only one neocortical study (Deuchars & Thomson, 1995*a*) to date, have attempted to determine directly which, if any, classes of interneurone activate $GABA_A$ or $GABA_B$ receptors selectively.

By combining dual intracellular recordings and biocytin filling, this study therefore aimed to describe the electrophysiological properties of single axon neocortical IPSPs in slices from mature rats under conditions that are as close to physiological as can be achieved *in vitro*. An important parallel aim was to determine whether IPSP properties could be correlated with presynaptic interneurone physiology and morphology.

METHODS

In early experiments, male Sprague–Dawley rats, 120–250 g in body weight, were anaesthetized with Fluothane and decapitated. Coronal slices of somatomotor cortex 400 μm thick were prepared in ice-cold, and incubated in warmed (34–36 °C), standard artificial cerebrospinal fluid (ACSF, see below). In later experiments, the rats were anaesthetized with Sagatal (sodium pentobarbitone, 60 mg kg^{-1} I.P.; Rhône Mérieux, Dublin, Ireland) and perfused transcardially with ice-cold ACSF in which the NaCl had been replaced with 248 mM sucrose and to which Sagatal (60 mg l^{-1}) was added. In the later experiments 500 μm-thick slices were used and

during slice preparation (ice-cold) and for the first hour of incubation in the recording chamber (34–36 °C), the slices were maintained in the sucrose-containing medium (without Sagatal) equilibrated with 95% O_2–5% CO_2. This was then replaced with standard ACSF (containing (mM): 124 NaCl, 25·5 $NaHCO_3$, 3·3 KCl, 1·2 KH_2PO_4, 1 $MgSO_4$, 2·5 $CaCl_2$ and 15 D-glucose) in which all recordings were performed. Recordings commenced after a further hour in this medium and the data presented here were obtained between 4 and 12 h after placing the slices in the bath.

Electrophysiological recordings

Intracellular recordings were made from pairs of superficial, or pairs of deep layer neurones with conventional sharp electrodes filled with 2 M $KMeSO_4$ (potassium methyl sulphate) and 2% w/v biocytin (100–150 MΩ) using an Axoprobe (Axon Instruments). Single spikes, pairs of spikes, or spike trains were elicited in the presynaptic neurone by injection of ramp and/or square-wave current pulses. The shape and amplitude of the pulse and its repetition rate could be modified according to the experimental design. Continuous analog recordings from both neurones were made on magnetic tape (Racal Store 4). Postsynaptic membrane potential was maintained within 2 mV of a preset value, and after sufficient data had been collected at one potential, could be changed. During continuous current injection, electrode balance was maintained by observing voltage responses to small, brief current pulses injected before or after responses to presynaptic spikes.

The properties of recorded cells were assessed from the voltage responses to 100 or 200 ms current pulses between −2·0 and +1·0 nA in amplitude, delivered from membrane potentials ranging from −65 to −80 mV. In early experiments, these data were stored on analog tape and analysed using a digital storage oscilloscope. In later experiments, neuronal responses to current injection were controlled and collected on disk using pCLAMP software (Axon Instruments).

Dual recording data were collected from tape to disk and analysed off-line (using in-house software: Thomson, Deuchars & West, 1993*a*; Thomson *et al.* 1995).

Each single sweep was then observed and either accepted, edited, or rejected according to the trigger point(s) that would trigger measurement or averaging of postsynaptic data during subsequent analysis. Acceptable, or adequately edited sweeps were those in which the rising phase of each presynaptic spike was recognised by the software as a trigger point. Editing consisted of removing false, or adjusting inaccurate, trigger points. Some additional sweeps in which postsynaptic baseline noise was unacceptable were also rejected.

IPSPs elicited by the first action potential in a train were analysed using the rising phase of the 1st spike to trigger data collection and analysis. Analysis of 2nd and 3rd spike responses required triggering of data analysis from the 2nd or 3rd spike. Numbers of spikes and interspike intervals were varied from sweep to sweep in some experiments. Sweeps were therefore selected into data subsets according to the number of presynaptic spikes, the interspike interval(s) and/or the duration of the presynaptic spike train. Illustrated averages of responses to brief trains of spikes are composites of: (i) averaged responses to single presynaptic spikes, (ii) averaged responses to pairs of presynaptic spikes at a preset interspike interval, and (iii) averaged responses to 3rd spikes, again at a preset interval. Two and three spike train IPSP integrals were measured as the area under the average IPSP obtained under stable conditions and normalized to the area under a single spike IPSP. These measurements were controlled by hand and artifacts excluded. IPSP 10–90% rise time was measured as the time taken for the IPSP to rise from 10 to 90% of its peak amplitude. IPSP width at half-amplitude was the time interval between the IPSP rising to 50% and then falling again to 50% of its peak amplitude.

In the figures, spike artifacts have simply been removed graphically after averaged responses had been computed and composites produced. Numbers given in the text are means ± S.D.S with the range in brackets.

Histological processing

Synaptically connected neurones and some other recorded interneurones were filled with biocytin by passing 0·5 nA depolarizing current in a 50% duty cycle at 1 Hz for 5–15 min (see also Deuchars & Thomson (1995*b*) for processing details).

After incubation for a further hour in the recording chamber, the slices were fixed overnight in a solution of 0·1 M phosphate buffer containing 1·25% glutaraldehyde, 2·5% paraformaldehyde and 15% picric acid. Slices were incubated in 20% sucrose in 0·1 M phosphate buffer for 30 min and freeze–thawed in liquid nitrogen before sectioning at 60 μm on a vibratome. Injected biocytin was localized with the Vector ABC kit and visualized using 3'3' tetraminodiaminobenzidine (Sigma) and the sections dehydrated and embedded in Durcupan resin (Fluka) on slides. Filled and recovered neurones were drawn in their entirety under a ×100 objective. When possible connections were observed the relevant areas were photographed and a second drawing was made that detailed only those postsynaptic dendrites and presynaptic axon collaterals that appeared to be involved in the synaptic connection. In addition to the recorded cell pairs, histological material that included a well-labelled interneurone axon was examined at the light level for putative contacts with other labelled neurones. These putative contacts and a random sample of additional boutons were also examined at the electron microscope (EM) level.

Material for electron microscopy was then processed further. The coverslip was removed from the slide and a portion of the 60 μm section containing a relevant area was cut from the resin and glued to a resin block. The edges of the block were trimmed with a razor blade until only the relevant areas remained. The block was then photographed and sectioned at 60–70 nm using a diamond knife (Microstar) on an Ultracut S microtome (Reichert). Sections were collected on copper grids with 1 mm or 0·5 mm slots coated with Formvar or Butvar (Sigma). The block was once again photographed. The sections were then lead stained and viewed on a Phillips 201 transmission or a Jeol 300X electron microscope fitted with a goniometer stage. Relevant areas were examined by reference to the photographs taken of the blocks before and after cutting.

Somata of the postsynaptic pyramidal targets of labelled interneurone axons were examined in their entirety at the EM level to ensure that inputs that might have been obscured by the peroxidase labelling at the light level were included.

RESULTS

Probability of inhibitory connections

In 100 experiments > 5000 neocortical neurones were recorded in layers II/III and V/VI. Of these, 275 cells were classifiable as non-pyramidal cells by their fast spiking properties, or by the IPSPs they elicited in simultaneously recorded pyramids. Of 595 dual recordings in which a non-pyramidal neurone was recorded simultaneously with a pyramidal neurone, thirty-nine yielded monosynaptic,

single axon IPSPs. This would give an average probability of each recorded interneurone innervating 1 : 15 of its closely neighbouring pyramidal partners. However, both slice thickness and preparation procedure appeared to affect this proportion. In the more recent studies in which 500 μm- (rather than 400 μm) thick slices were prepared from animals that had been perfused transcardially with ice-cold sucrose-containing ACSF, this probability rose to 7 : 32. In addition (see below) one connection shown at the ultrastructural level to involve two somatic boutons was missed during the recording, indicating that the recorded sample was biased towards the larger connections. That interneurones innervate one in four to five of their close pyramidal neighbours may therefore be a more realistic estimate.

Classification of interneurones

Classical fast spiking interneurones

Electrophysiological characteristics. Of the thirty-nine paired recordings, twenty-four were sufficiently stable for some of the properties of the IPSP to be studied. The interneurones that generated these IPSPs displayed a range of electrophysiological properties. Ten of the twenty-four could be classified as 'classical fast spiking interneurones'. These cells had a spike width at half-amplitude of $< 0{\cdot}5$ ms, displayed little or no spike accommodation or frequency adaptation and had predominantly linear current–voltage relations at membrane potentials negative to −65 mV. At more positive membrane potentials they displayed strong outward rectification. Perhaps the most striking and

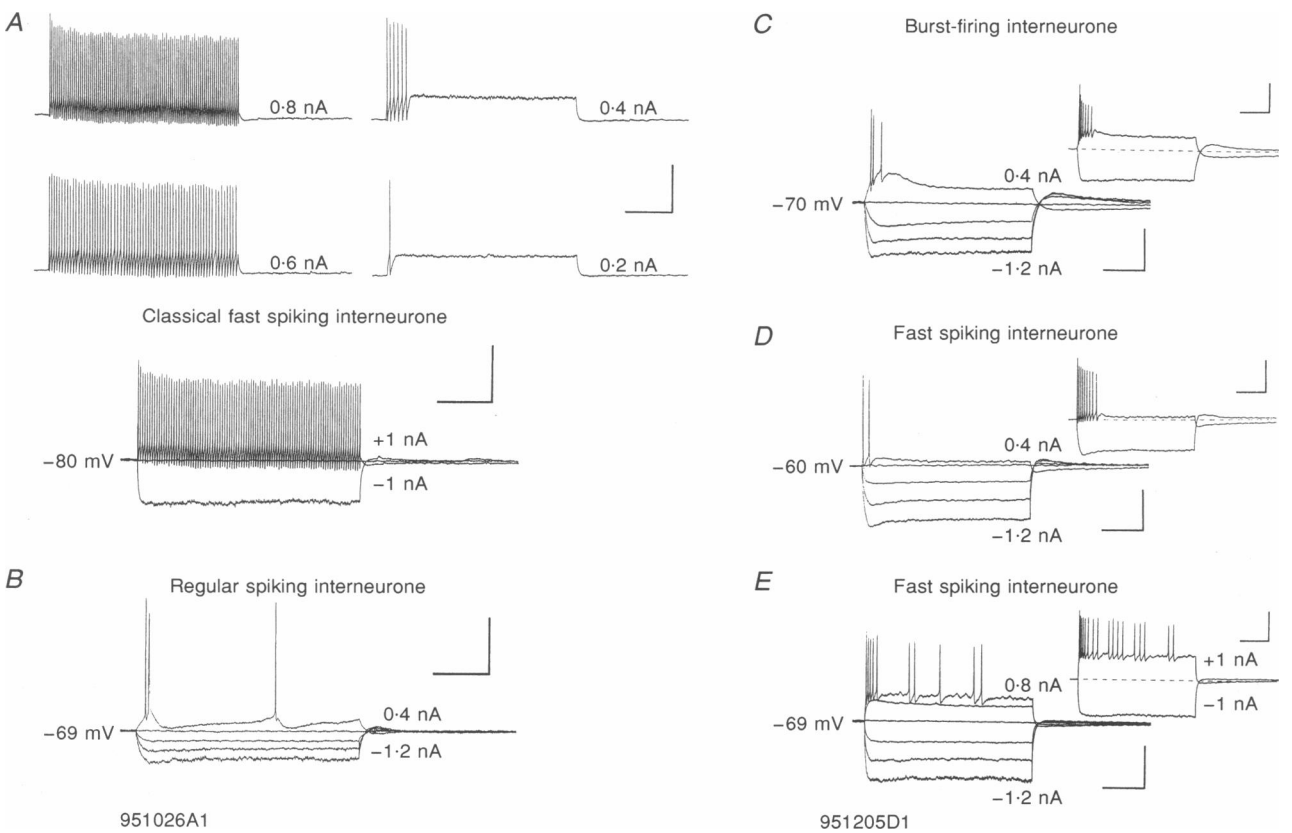

Figure 1. Electrophysiological characteristics of interneurones

A classical fast spiking interneurone (*A*), a regular spiking interneurone (*B*), a burst-firing interneurone (*C*) and two non-classical fast spiking interneurones (*D* and *E*) are shown. All traces illustrated are single sweep responses to 200 ms current pulses. The amplitude of the largest negative and largest positive pulse is given on each trace. Where 5 or 6 traces are superimposed, 0·4 nA separates the amplitude of each successive pulse. All scale bars are 40 mV and 50 ms. The insets in *C* and *D* show responses to +1 nA and −1 nA current pulses for comparison with the lower records in *A*. Cells *D* and *E* were not classified as classical fast spiking interneurones because *D* exhibited spike accommodation and *E* displayed a shallower AHP and less outward rectification at potentials positive of rest. Cell *C* was classified as burst firing because of the more pronounced inward rectification at negative potentials and the pronounced 'rebound' depolarization that followed negative current pulses and the less pronounced outward rectification at more positive membrane potentials. Moreover this cell was recovered histologically and was a spiny interneurone.

Table 1. Location of synapses made by neocortical classical fast spiking interneurones with labelled pyramidal cells

Reference number	Fig. nos		Location of synapses on identified pyramidal cells				Random synaptic target pattern			Layer location
	Anatomy	Physiology	Soma	Dendrite	Axon	Total	Soma	Dendrite	Spine	
930614A1	5,6	6	0	2	1	3*	5(29%)	12(70%)	0	V
930224B1	7*b*–9	7	0	5	0	5	3(17%)	15(83%)	0	V
930224(B1)	7*c*	—	2	0	0	2	—	—	—	V
930310	3,4	—	0	2	0	2	14(82%)	3(18%)	0	VI
930518(B1)	3	—	0	1	0	1	0	11(100%)	0	V
930406	2*A*	—	—	—	—	—	2(15%)	8(62%)	3(23%)	V
930525	2*C*	—	—	—	—	—	1(10%)	8(80%)†	1(10%)	V
931014	2*B*	—	—	—	—	—	2(12%)	12(70%)	3(18%)	V
Regular spiking cell axon										
951026(A1)	—	1,13	—	—	—	—	4(44%)	5(56%)	0	—

* Light microscopic estimate. † Autapse included. Synaptic connections made by classical fast spiking interneurones (and one presumptive regular spiking interneurone) with identified postsynaptic pyramidal neurones (numbers on left-hand side) and unidentified, randomly selected targets. A1/B1 associated with the cell reference number indicates that a recorded connection is documented here. Where this part of the reference number is in brackets, another postsynaptic target of this interneurone was recorded, but the synapses documented were with unrecorded partners. All connections documented here (except 930614A1, which was recorded but recovered only at the light microscope level) were confirmed at the EM level. Layer location: location of the interneurone soma in the somato-motor cortex.

distinguishing feature of this group of cells was, however, the depth of the spike AHP (15–25 mV) and its apparently monophasic decay (see Fig. 1*A*).

Morphological characteristics. All cells with these classical fast spiking characteristics that have been filled with biocytin and fully recovered histologically (7 cells, 3 of which elicited fast IPSPs in simultaneously recorded pyramidal neurones) had smooth, aspiny, beaded dendrites (see Table 1 and Figs 2–9). Their axons were partially myelinated and ramified extensively. However, the axonal arbours varied widely in shape and extent. Some innervated discrete regions of a single layer, others innervated both superficial and deep layers (see Figs 2, 3, 5 and 8). The boutons of these axons were frequently large (up to 2 μm in diameter) and contained large mitochondria (see Figs 2*D*, 4*C* and 9*E* and *B*). One 'autapse' was confirmed at the EM level, i.e. one of the interneurone axons innervated one of its own dendrites (see Fig. 2*C* and *D*).

Morphology of connections with reconstructed pyramidal cells. Table 1 summarizes the five classical fast spiking interneurone to pyramidal cell connections that were identified anatomically, i.e. in which both pre- and postsynaptic neurones were fully reconstructed anatomically. In two of these, the IPSP was also recorded (see Figs 5–9). Two of the anatomically demonstrable connections resulted from biocytin fills of pyramidal neurones that were recorded before the interneurone was penetrated (Figs 3 and 4). In one (930518, Fig. 3), a different pyramidal cell was subsequently recorded as a postsynaptic partner, but this second pyramid was not fully recovered. Interneurone 930224 (Figs 7–9) provided two confirmed somatic contacts to cell *c* (Fig. 7) and three putative contacts to cell *d* and was recorded simultaneously with pyramidal cells *b*, *c* and *d*. However, an IPSP was only apparent in the recording with cell *b* (see Fig. 7). Since the connection with pyramid *d* was neither recorded nor confirmed at the EM level only the contacts with cells *b* and *c* are included in Table 1.

Synaptic connections for four of the pairs (one recorded) were confirmed with electron microscopy (see Figs 3, 4 and 9) and involved one, two, two and five contacts, respectively. Confirmed synaptic contacts were with the apical dendrite, the basal dendrites, or with the soma, each pair involving synapses in only one of these compartments although a single interneurone could innervate the basal dendrites of one pyramid and the soma of another, e.g. interneurone 930224 (Fig. 7*b* and *d*). Although the three putative synaptic connections involved in the fifth pair (930614A1, Figs 5 and 6) could not be confirmed at the ultrastructural level, the light microscopic findings are included in Table 1 and illustrated because the connection was demonstrated electrophysiologically. Two of these putative contacts were with basal dendrites and one with the postsynaptic axon.

It is the connections with these fast spiking, smooth interneurones that form the basis of this paper. To place these events in a wider context, however, the cell properties and the IPSPs generated by other classes of interneurones are described briefly.

Two other classes of interneurones

Of the fourteen other presynaptic interneurones, eight were unclassified. The recordings from many of these unclassified, or slow interneurones were either too brief or of too poor a quality for the properties of the presynaptic neurone to be studied in any detail, but they did not resemble classical fast spiking cells in either narrow spike width or non-accommodating spike firing. Only one of these neurones has been fully reconstructed histologically and this was not one that was simultaneously recorded with a postsynaptic target. The soma of this neurone was in layer VI, its dendrites were beaded and had a small number of large diameter spines and the unmyelinated axon ramified in layers V and VI (not illustrated).

Three of the neurones that generated monosynaptic IPSPs were indistinguishable from pyramidal neurones in their electrophysiological properties (see Fig. 1*B*). Again, none of these cells has to date been fully reconstructed. However, following the recordings illustrated in Fig. 13, a labelled interneurone axon was observed to ramify extensively in the recorded region (not illustrated, see Table 1 for the targets of this axon). Furthermore, when the IPSP illustrated in Fig. 13 was challenged with DNQX (6,7-dinitroquinoxaline-2,3-dione, 20 μM, for >30 min), this excitatory amino acid antagonist did not depress the IPSP, while bicuculline (5 μM) reduced it by 80% in 10 min (not illustrated, see also below Disynaptic IPSPs).

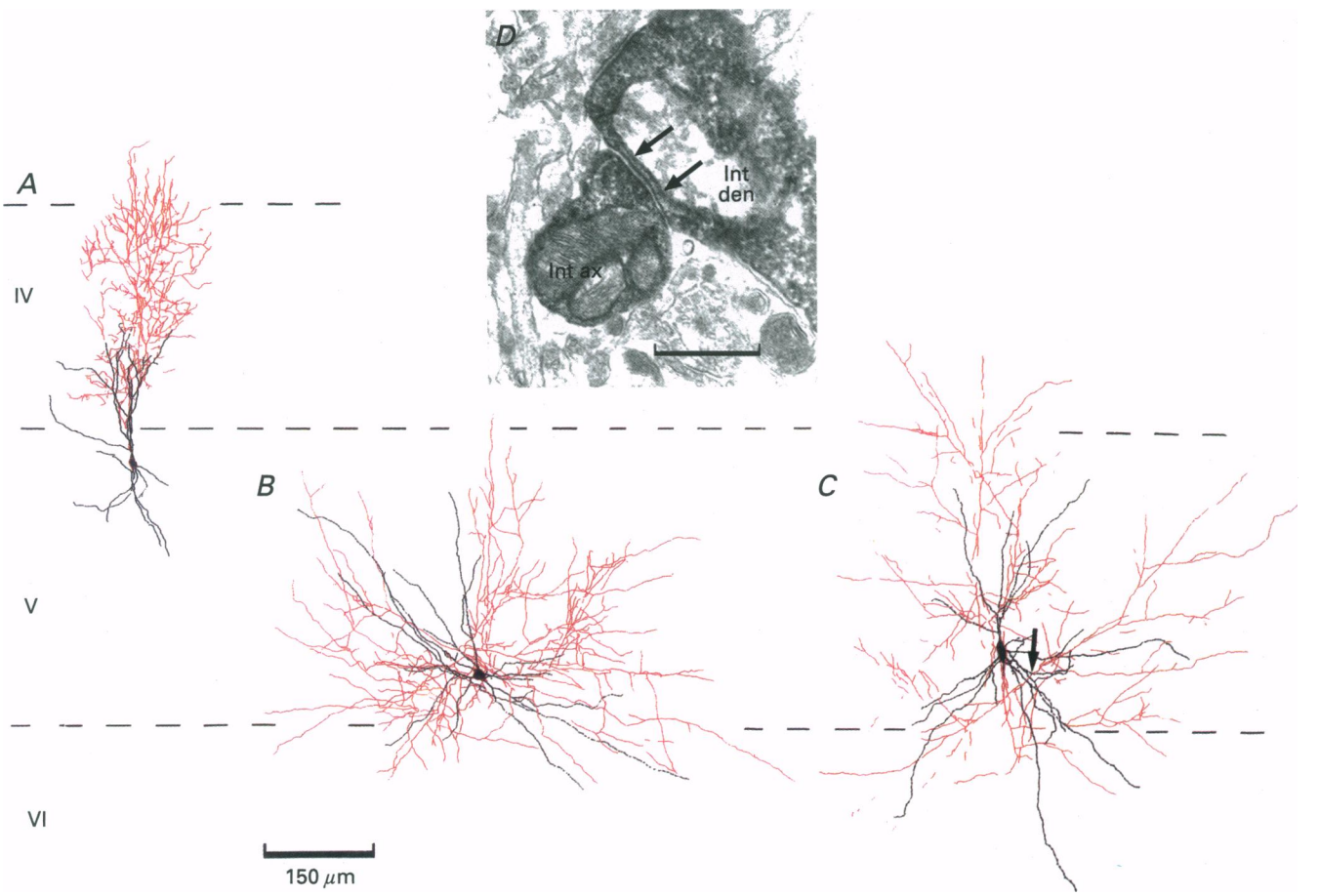

Figure 2. Axonal arborization of three infragranular classical fast spiking interneurones

Somata and dendrites are illustrated in black and axons in red. In *A* the only classical fast spiking cell with dendrites that were not uniformly beaded is illustrated (930406). The axon of this neurone was fully reconstructed from 3 sequential 60 μm-thick sections, but the arborization was so dense that the axon contained in only one of these sections is illustrated. The entire arbour was contained within the same dorso-ventral and medio-lateral area illustrated and extended about 150 μm rostro-caudally. In *B* (931014) and *C* (930525), the entire labelled axonal arbours for two other interneurones are illustrated. The interneurone in *C* innervated its own dendrite; see arrow in *C* and electron micrograph *D*. In *D*, Int ax and Int den label the interneurone axon and dendrite, respectively. The arrows in *D* point to the region of synaptic specialization identified by rigid apposition of pre- and postsynaptic membranes and thickening of the postsynaptic membrane. The scale bar in *D* is 0·5 μm.

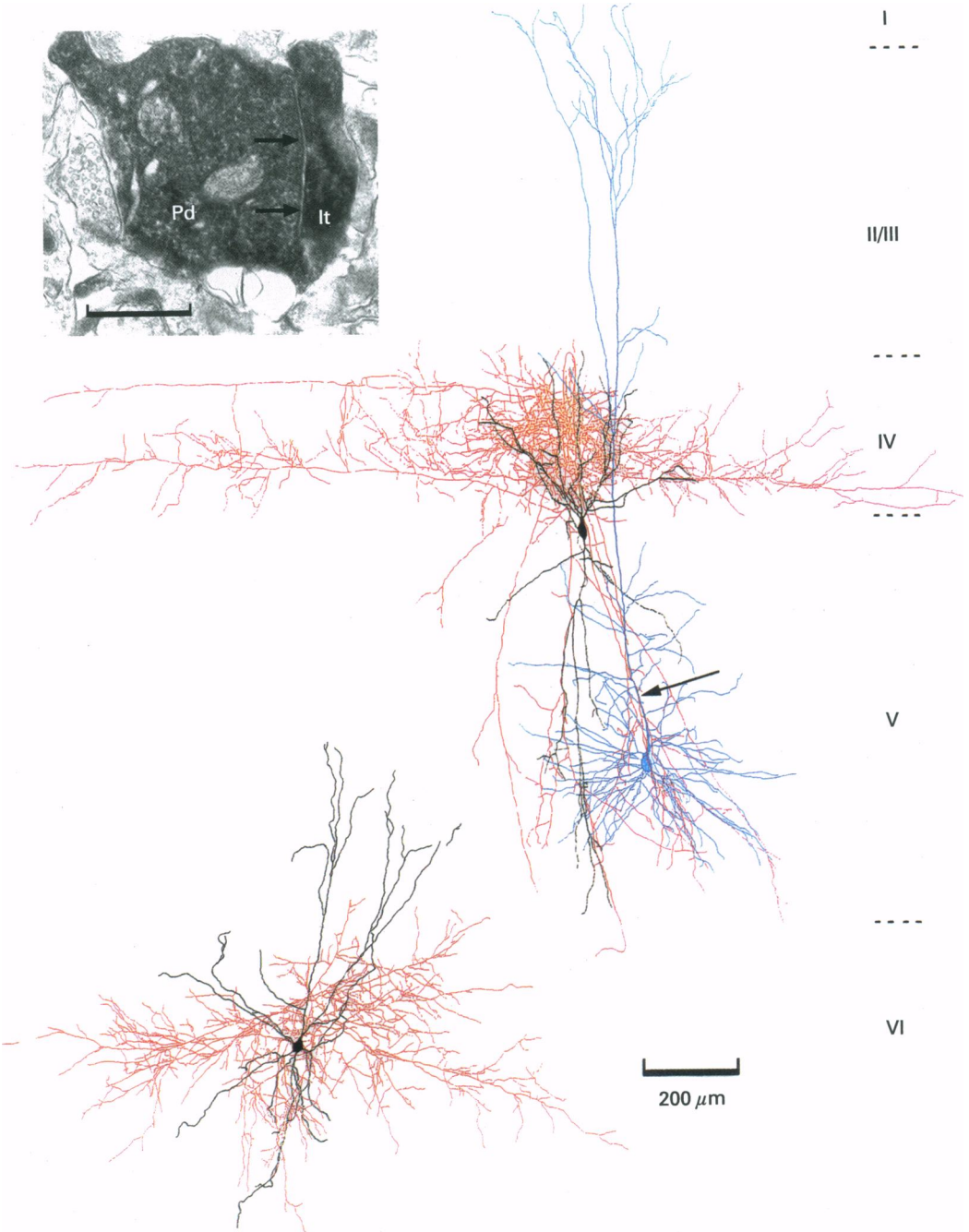

Figure 3. Axonal arbours of two infragranular classical fast spiking interneurones

Interneurone somata and dendrites are drawn in black and their axons in red. The soma and dendrites of a postsynaptic target of one of these interneurones (930518) are also drawn, in blue. In this pair, the presynaptic interneurone soma was in upper layer V and it had an extensive axonal arborization in layer IV. The soma of the postsynaptic pyramidal cell was located deeper in layer V and its apical dendrite extended to form an apical tuft in layer I. The single synapse involved in this connection is indicated by the arrow on the drawing and illustrated in the electron micrograph. In the micrograph, Pd and It label the pyramidal dendrite and interneurone axon terminal, respectively. The arrows point to the region of synaptic specialization. The interneurone located in layer VI (930310) had an extensive axonal arbour that was largely restricted to layer VI. This interneurone made two synaptic contacts with the basal dendrites of a pyramidal cell whose soma was located in upper layer VI. These connections are illustrated in Fig. 4. The scale bar for the micrograph is 0·5 μm.

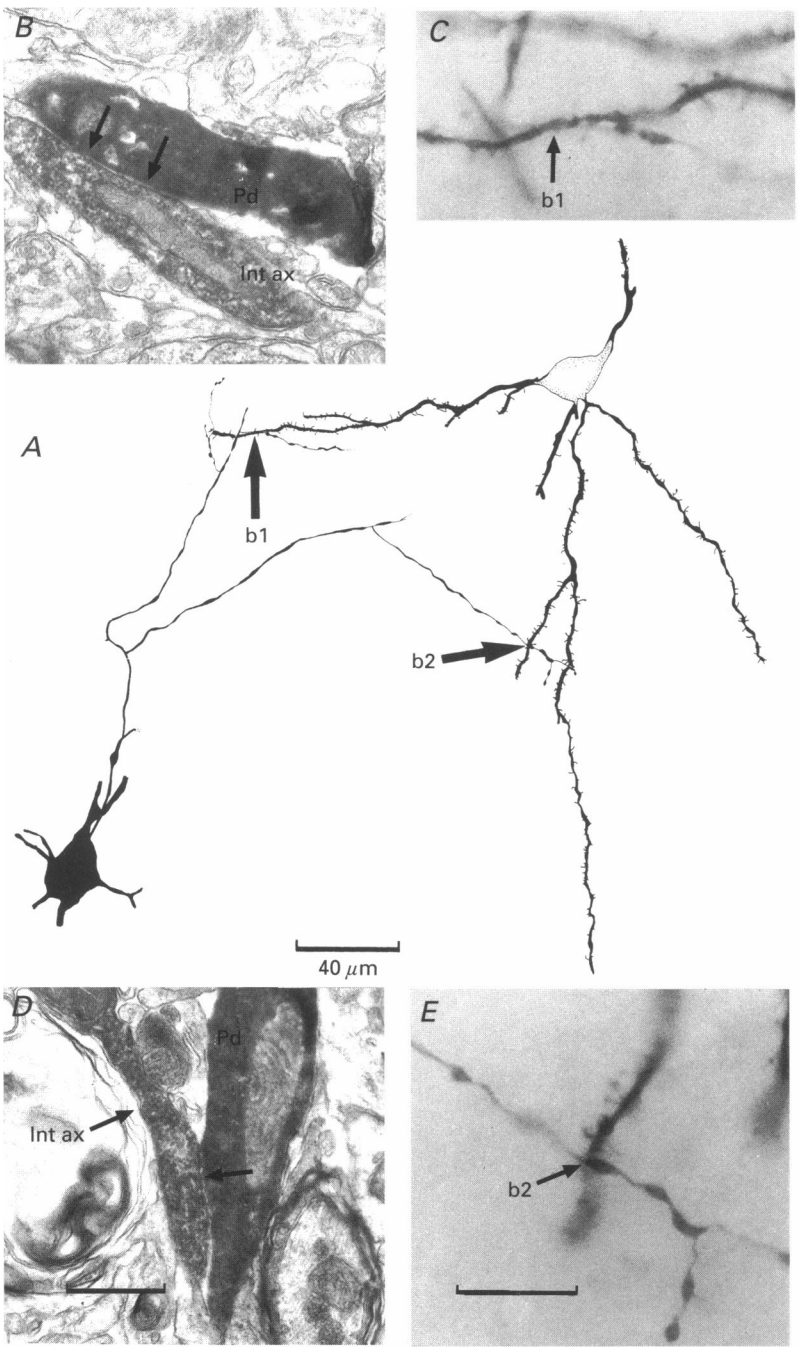

Figure 4. A classical fast spiking interneurone located in layer VI (930310) and illustrated in Fig. 3, makes two synaptic contacts with two basal dendrites of a pyramidal neurone whose soma is in upper layer VI

In *A*, a drawing tube reconstruction illustrates the locations of the two synapses (b1 and b2) and the relative positions of presynaptic interneurone soma (filled in black) and postsynaptic pyramid (soma stippled). Only those portions of the interneurone axon and pyramidal dendrites contributing to these connections are drawn. Bouton b1 is illustrated at the electron and light microscopic levels in *B* and *C*, respectively, and the input b2 in *D* and *E*. The scale bar in *D* (0·5 μm) is the same as for *B*. The scale bar in *E* (15 μm) also applies to *C*. In *B* and *D*, Int ax and Pd label interneurone axon and pyramidal dendrite, respectively. The other arrows point to the regions of synaptic specialization.

Non-classical fast spiking interneurones

The remaining three presynaptic interneurones all had fast spikes (width at half-amplitude < 0·5 ms), but displayed more complex voltage relations than 'classical fast spiking cells' (see Fig. 1*C* and *D* for cells that would be classified as non-classical fast spiking interneurones). There was, for example, some delayed inward rectification at negative membrane potentials, typically less outward rectification at potentials positive of rest and these cells exhibited both spike accommodation and frequency adaptation. The spike AHP was also shallower (< 10 mV) than in classical fast spiking cells. One of these cells (Fig. 1*D*) could be characterized as a burst-firing, or low threshold spiking neurone from its electrophysiological characteristics (Kawaguchi & Kubota, 1993) and was shown to be a sparsely spiny interneurone on histological reconstruction. However, since these spiny interneurones (Thomson *et al.* 1995; Deuchars & Thomson, 1995*b*) and the IPSP generated by one of these in the superficial layers have been described previously (Deuchars & Thomson, 1995*a*), they are not illustrated here. The morphological characteristics of the other non-classical fast spiking cells have yet to be fully described.

Amplitude, time course and voltage sensitivity of single axon IPSPs

At −55 to −60 mV, average IPSP amplitude and time course varied widely amongst the twenty-four IPSPs studied (amplitude, 0·20–3·5 mV; rise time, 1·4–10 ms; width at half-amplitude, 8 to > 100 ms). Extrapolated IPSP reversal potentials were between −68 and −83 mV ($n = 11$) and IPSPs increased in average amplitude by between 30 and 150% with a 10 mV postsynaptic depolarization (slope). To determine whether the smaller amplitudes and slower

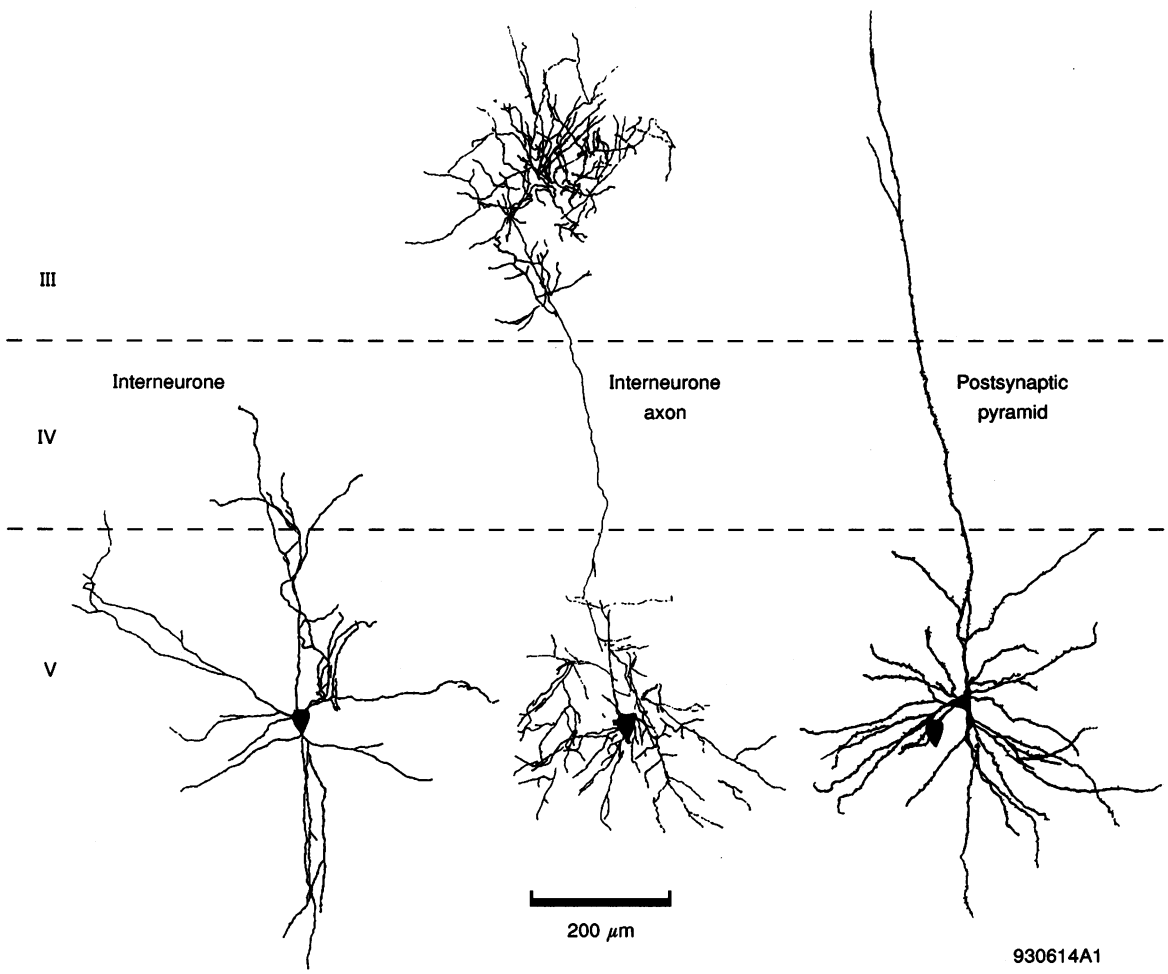

Figure 5. Drawing tube reconstruction of a layer V, classical fast spiking interneurone that was recorded simultaneously with a postsynaptic layer V pyramidal cell (930614A1)

For clarity the interneurone soma and dendrites, the interneurone axon and the pyramidal cell soma and dendrites are each drawn separately. The interneurone soma was located slightly ventral and to the left of the pyramidal soma and its position is indicated on the right-hand side drawing of the pyramid. Figure 6 illustrates more detailed morphology and physiology of this connection.

time courses could be due to filtering of IPSPs more distal to the soma, attempts were made to obtain correlations between these parameters. However, the only correlation found to be significant was that between IPSP rise time and width at half-amplitude. The IPSPs with faster rise times also had narrower widths at half-amplitude. However, the fastest IPSPs were not necessarily those with the largest amplitudes, nor were they the most sensitive to changes in somatic membrane potential. The two IPSPs for which the presynaptic axon and postsynaptic pyramid were fully reconstructed were two of the smallest IPSPs studied (< 0·4 mV at −55 mV, not included in Table 2) and involved three (putative, Fig. 6) and five (confirmed, Fig. 9) boutons, respectively. Latencies were invariant (or variations were

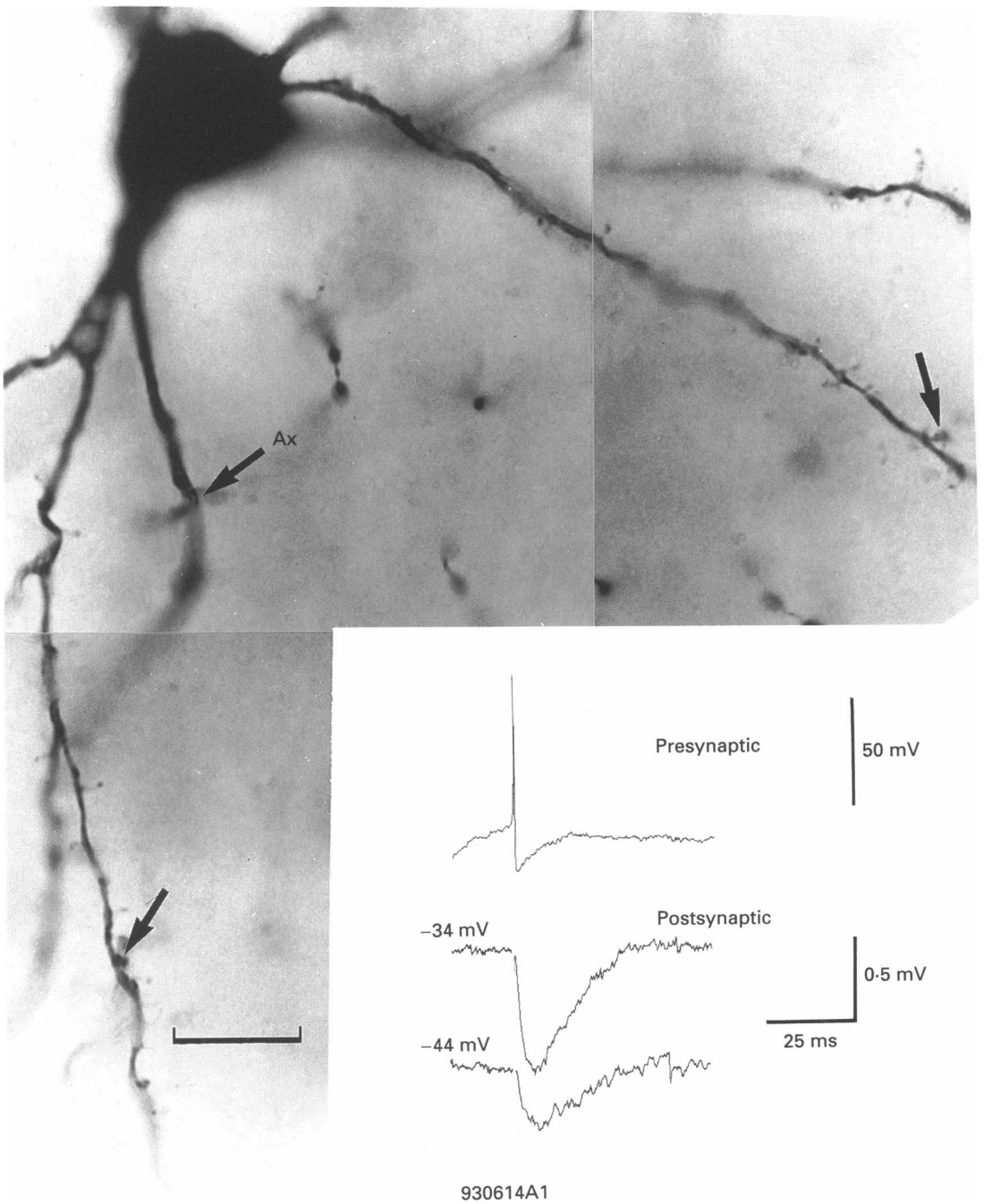

Figure 6. Light microscopic photomontage of the pyramidal cell that was postsynaptic to the classical fast spiking interneurone illustrated in Fig. 5 (930614A1)

Three putative synaptic contacts are marked with arrows. Two contacts are with basal dendrites and one with the axon (Ax). The physiology of this connection is illustrated in the inset. Averaged postsynaptic responses to single presynaptic action potentials, recorded at two membrane potentials, are illustrated (> 100 sweeps each average). In this and similar figures, spike artifacts have been removed graphically after averaging. Scale bar in micrograph is 15 μm.

within the noise) and brief, between 1 and 2 ms, and were not correlated with IPSP time course.

There was some correlation between the 'type' of presynaptic interneurone and the properties of the IPSP it elicited. Broadly speaking, the slowest IPSPs were elicited by the unclassified interneurones and the fastest by the fast spiking interneurones (both classical and non-classical), with regular spiking interneurone IPSPs displaying intermediate rise times and half-widths (see Table 2 and Fig. 10). The amplitude of the IPSP was not, however, correlated with the type of presynaptic interneurone. In addition, the one burst-firing interneurone included in this study generated a

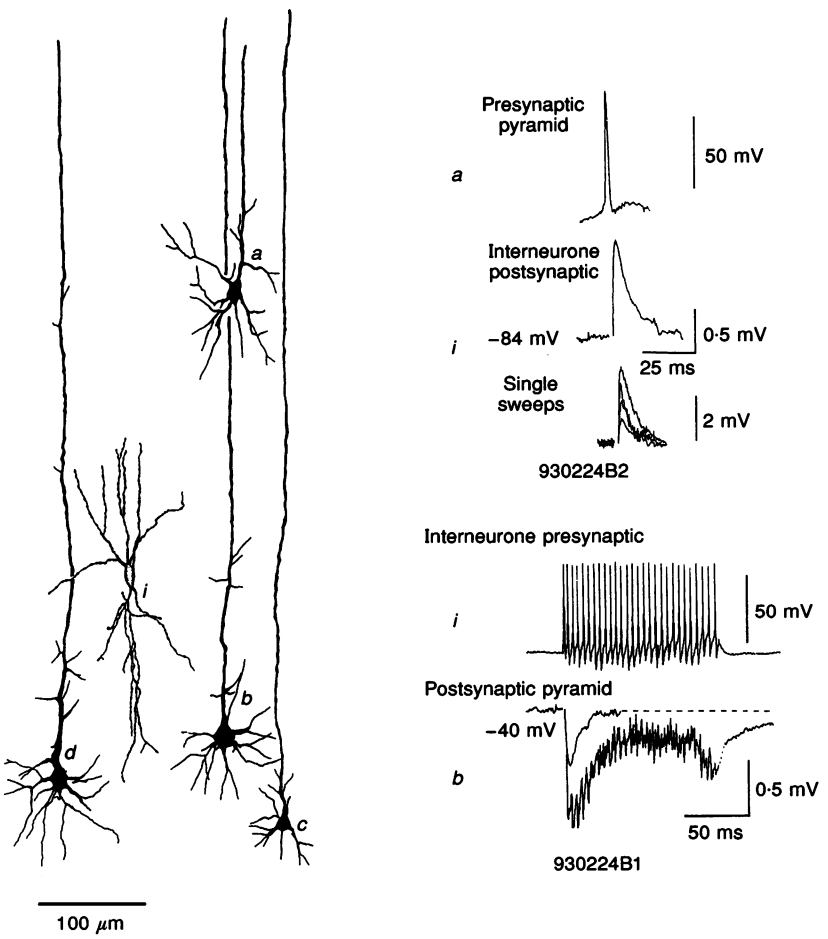

Figure 7. Low power drawing tube sketch of the somata and major dendrites of a classical fast spiking interneurone (930224B1/2)

The soma of the cell was in layer V (*i*), the pyramidal cell in lower layer III (*a*) was presynaptic to the interneurone (see recordings in upper inset) and three pyramidal neurones were postsynaptic to the interneurone (*b–d*). An attempt was made in this drawing to represent the absolute distances between the somata, since, for example, the soma of *i* was not in the same 60 μm section as (and was therefore a different rostro-caudal position from) pyramids *b* and *d*. Pyramids *b* and *d* were in layer V, and *c* in upper layer VI. Although all three postsynaptic pyramidal neurones were recorded simultaneously with the interneurone, only in the recording with *b* was an IPSP apparent (see lower inset for recordings). Electron microscopic analysis of *c* revealed 2 somatic synapses (not illustrated), but it was not possible to examine the 3 putative basal dendritic contacts with *d* at the EM level. Full light and electron microscope reconstructions of the connection with cell *b* are shown in Figs 8 and 9. In the upper inset, the EPSP elicited in the interneurone by single spikes in pyramidal cell *a* are illustrated. The middle record shows an averaged postsynaptic response (150 sweeps), the lower records are single sweep responses. Note that the average amplitude of the EPSP is only 1 mV. Single sweep responses were between 0 mV (i.e. failures) and 3 mV in amplitude. The lower inset shows the responses elicited in pyramidal cell *b* by the interneurone. Two averaged postsynaptic responses are superimposed below, the responses to single presynaptic action potentials (50 sweeps) and the responses to long trains of spikes (10 sweeps, see presynaptic record for a typical presynaptic spike train), both recorded at a postsynaptic membrane potential of −40 mV. Responses to trains of spikes were 3 point averaged to reduce spike artifact contamination of records. Note the slow decay of the responses to spike trains.

fast IPSP (similar to that described previously by Deuchars & Thomson, 1995*a*) whose time course was similar to that of fast spiking interneurone IPSPs. However, unlike these IPSPs, those generated by burst firing interneurones were never apparent with postsynaptic somatic recordings. The two recorded to date involved a dendritic postsynaptic recording site.

Voltage relations of single axon IPSPs

IPSP amplitude was found to depend not only on the membrane potential at which the IPSP was recorded, but upon the holding potential that preceded the test potential (see Fig. 10*C*). The more positive the holding potential, the more positive was the measured extrapolated reversal potential and the smaller the IPSP elicited. Measurements were therefore made within 1–2 min of a change from a set holding potential (between −60 and −70 mV for the population) and extrapolated reversal potentials are given in Table 1. All classes of IPSP reported here appeared similarly sensitive to current injected at the soma; however, only in one regular spiking interneurone IPSP and one unclassified interneurone IPSP was this more careful protocol for obtaining the reversal potential followed. Only the data for these two IPSPs are therefore included in Table 2. Attempts were also made to trigger IPSPs following a rapid step change in postsynaptic membrane potential from a preset holding potential. These experiments ($n = 5$) gave essentially similar results, but data analysis was confounded by the time-dependent activation of voltage-dependent currents in the postsynaptic pyramidal cell and is not illustrated here.

Fluctuations in classical fast spiking interneurone IPSP amplitude and shape

These IPSPs fluctuated in amplitude above baseline noise. Only in fast spiking interneurone IPSPs with an average amplitude < 1 mV (at −55 to −60 mV) were clear failures of transmission seen (single spikes at 0·33 Hz). IPSP amplitude histograms were constructed for four of the larger IPSPs for which > 300 spike-triggered IPSPs were elicited under

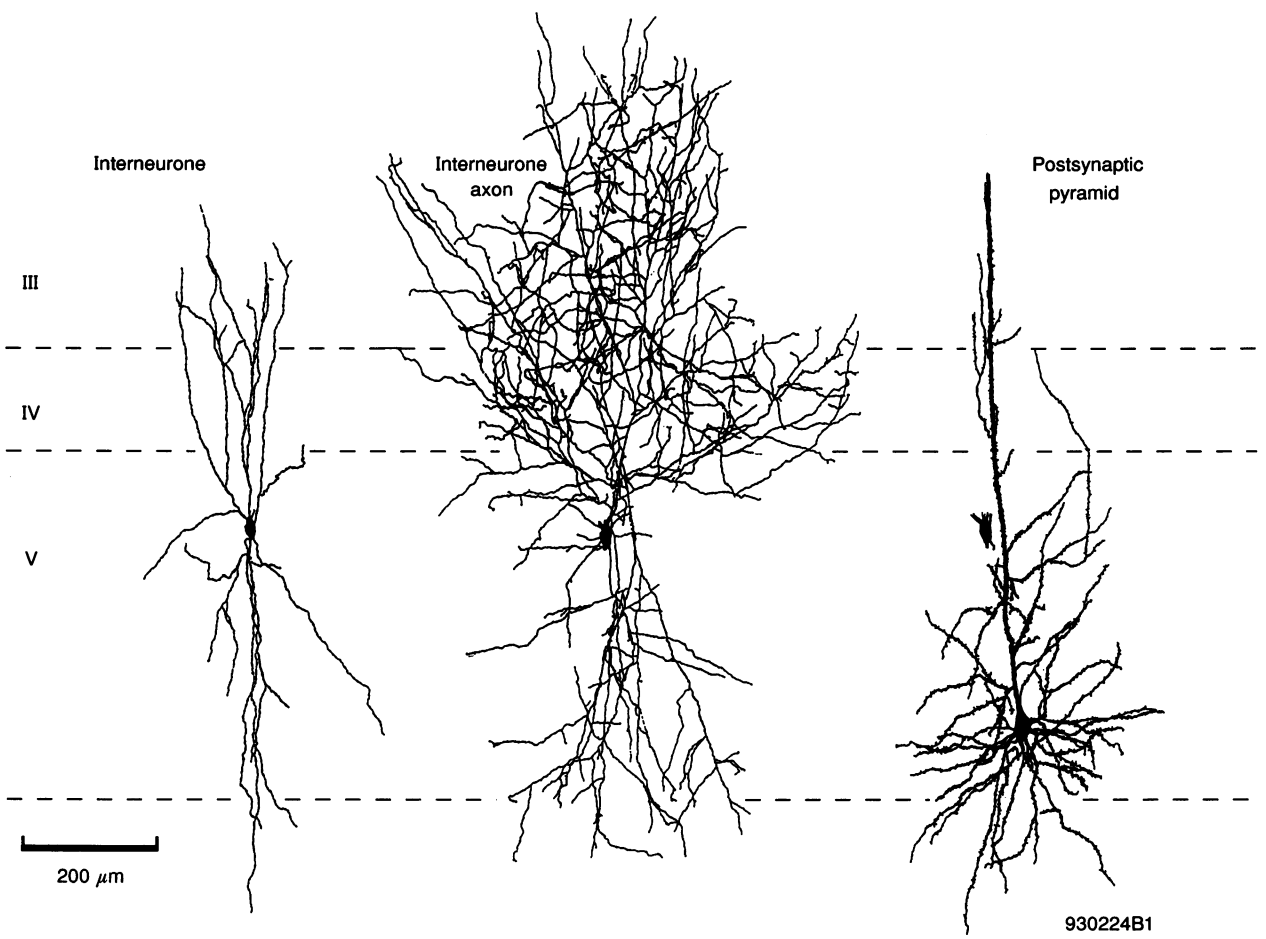

Figure 8. Drawing tube reconstruction of the layer V classical fast spiking cell and the postsynaptic pyramidal cell *b* illustrated in Fig. 7 (930224B1)

The soma and dendrites of the interneurone (left-hand side), its axonal arbour (middle) and the soma and dendrites of the postsynaptic pyramid (right-hand side) are each drawn separately for clarity. The position of the interneurone soma can be seen on the drawing of the pyramid to the left of the apical dendrite. In this drawing no correction for rostro-caudal differences was made.

Table 2. Properties of single axon IPSPs

	IPSP amplitude (mV)	10–90% rise time (ms)	Width at half-amplitude (ms)	Reversal potential (mV)	Change in amplitude with 10 mV depolarization (%)
Classical fast spiking interneurone ($n = 10$)	1·22 ± 0·71 (0·24–2·21)	2·71 ± 0·60 (1·8–3·7)	14·72 ± 3·83 (10–20)	−72·86 ± 6·92 (−71 to −82) ($n = 7$)	73·17 ± 38·71 (53–158) ($n = 7$)
Regular spiking interneurone ($n = 3$)	1·65 ± 1·32 (0·54–3·5)	3·77 ± 0·88 (3–5)	27·3 ± 3·68 (25–32)	−70 — ($n = 1$)	87 — ($n = 1$)
Unclassified interneurone ($n = 8$)	1·42 ± 0·74 (0·2–2·8)	6·3 ± 2·22 (3·1–10)	56·29 ± 23·44 (19·5 to >100)	−77 — ($n = 1$)	48 — ($n = 1$)

Properties of averaged IPSPs triggered by action potentials in one interneurone and recorded in a postsynaptic pyramid. Interneurones were classified as 'Classical fast spiking', 'Regular spiking', or were 'Unclassified' depending on their electrophysiological properties. IPSP amplitudes, 10–90% rise times and widths at half-amplitude were measured at postsynaptic membrane potentials between −55 and −60 mV (IPSPs recorded only at other membrane potentials are excluded). Reversal potentials and slopes were obtained from plots of IPSP average amplitude against postsynaptic membrane potential for at least 2 different membrane potentials. Means ± S.D.s are given with the range in brackets. Where n differs from the population, it is given below. Fast spiking interneurones that differed from classical fast spiking interneurones generated IPSPs similar to classical fast spiking types but are excluded from this table.

stable conditions (postsynaptic membrane potential held within 1 mV of a preset value and a stable presynaptic firing rate < 0·4 Hz). These were evenly distributed about the mean, only partially overlapped the noise distribution and no clear peaks were visible in the distribution. In two examples, a narrower distribution (i.e. one with a lower coefficient of variation) was obtained when IPSPs elicited at a more negative membrane potential were analysed. This would be consistent with a reduction in quantal amplitude at potentials closer to the reversal potential. Fluctuation analysis was not extended, however. One prerequisite for such analysis is that the shape of the event does not vary from trial to trial even when the amplitude fluctuates, so that the peak amplitude for each event is measured at the same point in time. While IPSPs elicited at more negative membrane potentials were relatively consistent in shape from trial to trial (see −68 mV records in Fig. 10), these were small in amplitude and often superimposed on electrode noise. Events elicited at more depolarized potentials were larger, but very much less consistent in shape. This is illustrated in Fig. 10*B* in which the standard deviation time course (SDTC) has been scaled to match the peak amplitude of the averaged IPSP and superimposed. The SDTC for the IPSP recorded at −56 mV clearly demonstrates a peak fluctuation after the peak of the average voltage response. This indicates that the peak and decay of the IPSP were inconsistent from sweep to sweep. It should be noted that the relative amplitudes of the SDTC and averaged IPSP might be taken to imply that the coefficient of variation would be greater at more depolarized potentials. However, the large baseline biological noise levels at membrane potentials close to firing threshold partially obscures the IPSP fluctuations under these conditions.

Responses to pairs and trains of presynaptic action potentials

Brief trains of classical fast spiking interneurone IPSPs

Classical fast spiking interneurones can maintain high frequencies of firing. The effects of pairs or trains of presynaptic spikes elicited at one train per 3 to 5 s were therefore tested in thirteen of the IPSPs, nine involving classical fast spiking interneurones (see Fig. 11 and filled circles in Fig. 12) and for comparison two involving regular spiking interneurones (open triangles and half-filled triangles in Fig. 12) and two involving unclassified interneurones (inverted filled triangle in Fig. 12). To obtain the data illustrated in Fig. 12, IPSPs were elicited at a steady postsynaptic holding potential by single presynaptic spikes interspersed with spike pairs and with brief spike trains. Interspike intervals and train durations were selected during off-line analysis and subsets of data used for each average produced. Averages comprising at least 50 and up to 200 IPSPs for each train duration were analysed and compared with averaged IPSPs elicited by single spikes. Care was taken to ensure that the averaged single spike IPSPs used for normalization were of the same amplitude as IPSPs elicited by the first spike of pairs or trains of spikes.

With spike pairs at interspike intervals < 10 ms (7 cell pairs) and again at intervals between 20 and 60 ms (3 cell pairs) IPSPs elicited by classical fast spiking interneurones displayed paired pulse depression (see larger filled circles,

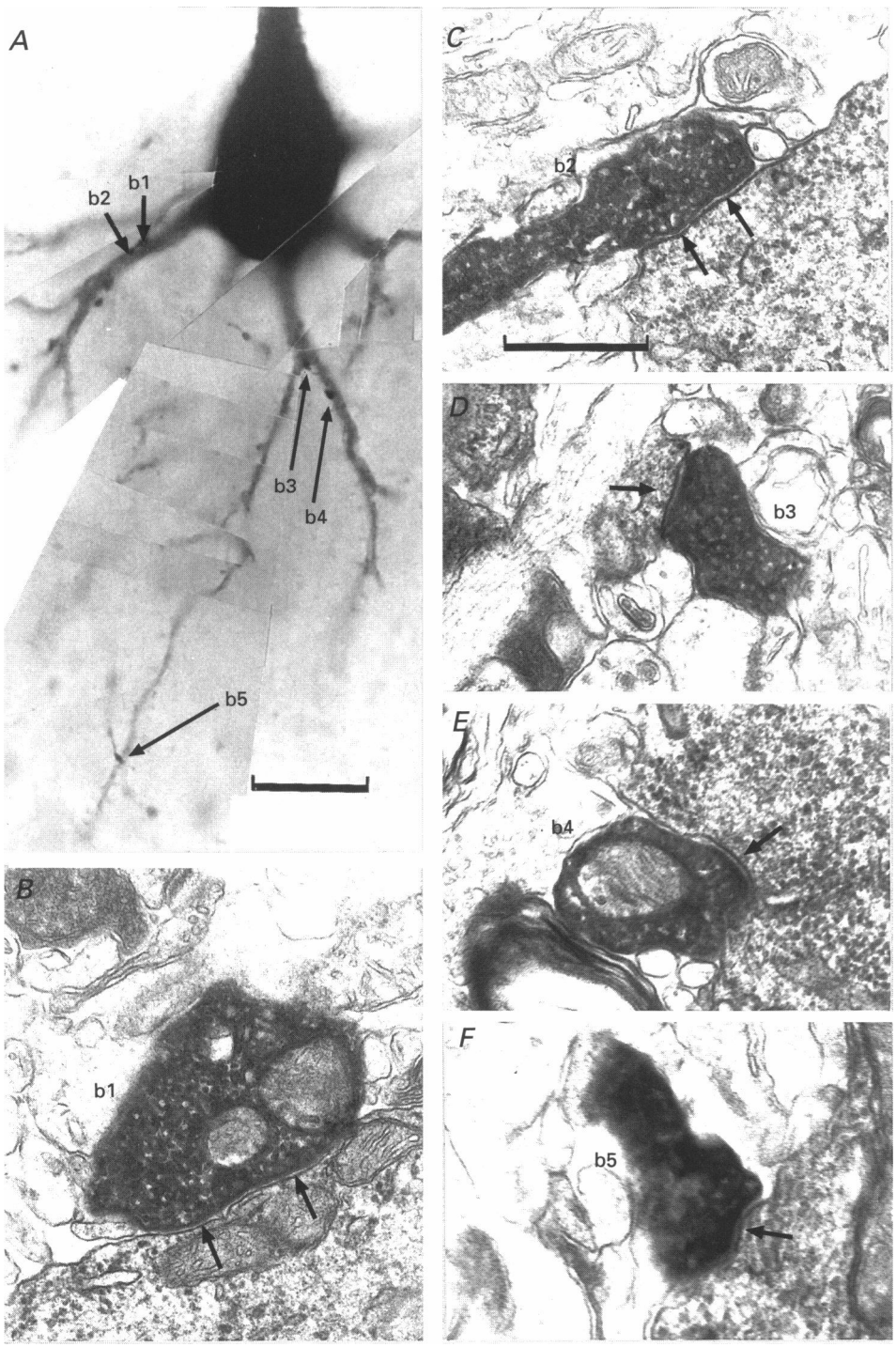

Figure 9. Light and electron microscopic reconstruction of interneurone to pyramid connection

Correlated light and electron microscopic reconstruction of the classical fast spiking interneurone to pyramid pair illustrated in Figs 7 and 8 (930224B1) revealed that the interneurone made 5 synaptic contacts with the basal dendrites of the postsynaptic pyramidal cell (cell *b* in Fig. 7). *A*, light microscopic photomontage of the postsynaptic pyramid with the locations of inputs from the interneurone labelled with the arrows (b1–b5). *B–F* show these same boutons at the electron microscopic level. Arrows mark regions of postsynaptic specialization. In each case the postsynaptic element is less strongly labelled than the presynaptic. In *B*, the synaptic specialization is not as evident as in *C–F*; however, this was considered to be a synapse because there was some thickening of the postsynaptic membrane and this bouton did not form synapses with any other structures. Scale bar in *A* is 20 μm. Scale bar in *C* is 0·25 μm and also applies to *B–F*.

Fig. 12). The integrated area under the averaged two spike IPSP was consistently less than twice the area under the averaged single spike IPSP. Only at interspike intervals between 10 and 20 ms was paired pulse facilitation apparent (3 cell pairs). Both large (2·2 mV) and small (0·2 mV) IPSPs demonstrated this facilitation and these IPSPs also exhibited paired pulse depression at both longer and shorter interspike intervals (see points marked by open and filled arrowheads for two examples, Fig. 12). No attempt was made to study longer intervals systematically.

The areas under three-spike IPSPs are also plotted in Fig. 12 (smaller symbols). Summing three-spike IPSPs could achieve a larger peak voltage change than two-spike IPSPs with the same train duration. The higher the firing frequency the larger the peak voltage (see Fig. 11). However, when IPSPs were compared for train durations < 20 ms, the areas under the three-spike IPSPs were only marginally larger than those under two-spike IPSPs. Adding a 3rd spike within the same time window did not therefore greatly increase the total area under the IPSP. The integral only increased significantly when the train duration was also increased. With longer train durations the 3rd IPSP added significantly to the response, but with trains up to 70 ms in duration three-spike IPSPs did not achieve 3 times the area under a single-spike IPSP. This was the case even when the interval between the 1st and 2nd or the 2nd and 3rd spikes was > 50 ms (for an example see Fig. 11*A*). Despite these results, the larger IPSPs rarely failed, even with the briefest interspike intervals.

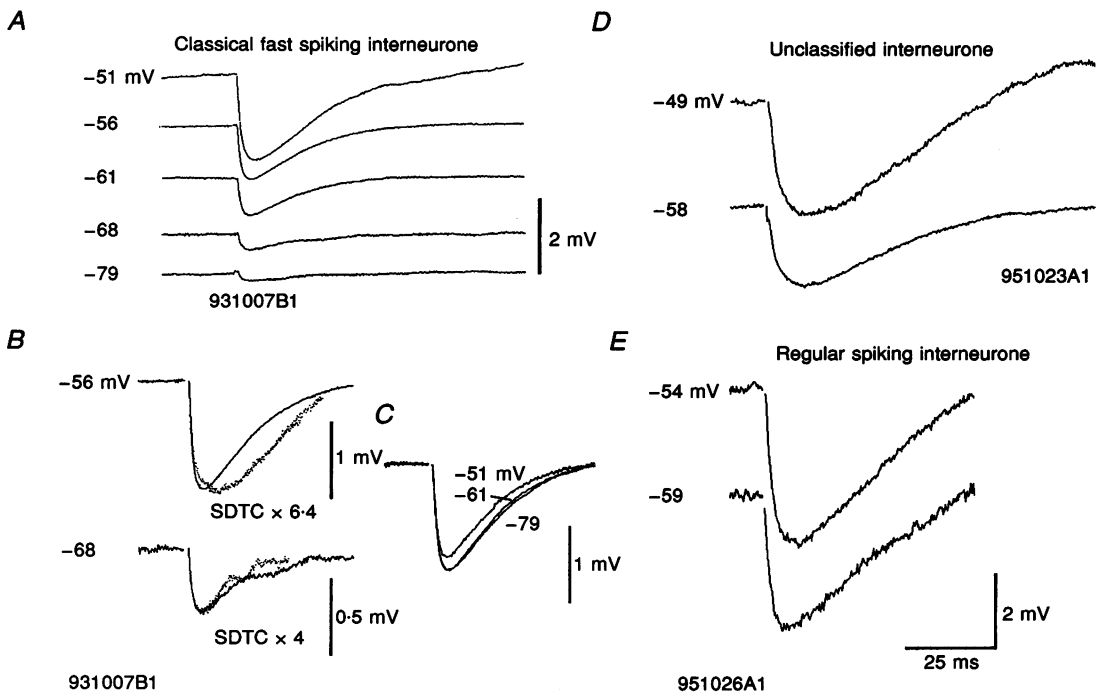

Figure 10. Averaged IPSPs triggered by single spikes

A–C, a classical fast spiking interneurone; *D*, an unclassified, or slow, interneurone; and *E*, a regular spiking interneurone recorded in three different pyramidal cells. Code numbers for each pair are given below the traces. Each postsynaptic response illustrated is the average of between 30 and 90 sweeps. IPSPs recorded at 5 (*A*) and 2 (*D* and *E*) different postsynaptic membrane potentials are illustrated. The time scale applies to all traces and the 2 mV voltage scales in *A* and *E* also apply to *D*. For the data illustrated in *A* responses at −51 mV were measured first, then −56 mV and so on with −79 mV last. The extrapolated reversal potential from the first two averages was close to −60 mV, but increased to > −70 mV when the holding potential was more negative than −60 mV. Finally, as apparent in the −79 mV trace, the reversal potential had become more negative than −80 mV. In *B* the IPSP also illustrated in *A* is shown at higher gain at two membrane potentials. Superimposed on the averaged response is the standard deviation time course (SDTC, dotted lines) scaled to match the peak average amplitude (and inverted). Note that the SDTC follows the shape of the averaged IPSP beyond its peak at −68 mV, but not at −56 mV. In *C*, 3 averages, all recorded at a membrane potential of −56 mV, are shown superimposed. Each average was obtained within 1–2 min of a change from the holding potential indicated to the right. The smallest average was obtained after the cell had been held at −51 mV for 10 min, the largest after holding the membrane at −79 mV for 10 min.

Regular spiking interneurones

The firing characteristics of regular spiking interneurones precluded detailed study of very brief interspike intervals or long trains. Like pyramidal cells, these interneurones would produce a relatively brief interval pair of spikes at the start of a depolarizing current pulse, but then exhibited strong frequency accommodation. Two IPSPs elicited by these interneurones displayed paired pulse depression at all interspike intervals studied between 5 and 65 ms (large open and half-filled triangles, Fig. 12). This depression appeared to decline as intervals increased. Some effect of postsynaptic holding potential was observed. In one cell pair, similar interspike intervals were studied at three holding potentials (−50, −53 and −58 mV; see half-filled triangles, Fig. 12). Paired pulse depression was reduced at the more depolarized potentials. In these IPSPs the 3rd spikes appeared to add significantly to the response at all intervals studied (see small open and half-filled triangles, Fig. 12), but again, did not achieve 3 times the area under a single spike IPSP.

Unclassified, or slow interneurones

Neither very short interspike intervals, nor long spike trains could be studied with unclassified or slow interneurones. At interspike intervals between 10 and 20 ms, the two IPSPs studied displayed paired pulse facilitation similar to that observed with classical fast spiking interneurones. However, a three-spike train (60 ms duration) elicited an IPSP only slightly larger than the two spike IPSP (15 ms duration) in one of these pairs (see filled inverted triangles, Fig. 12).

Longer spike trains in classical fast spiking interneurones

In classical fast spiking interneurone IPSPs, longer trains of action potentials elicited summing IPSPs. The peak amplitude achieved increased with presynaptic firing frequency up to more than twice the amplitude of a single-spike IPSP (at around 250 Hz). The averaged voltage envelope thereafter declined during the train, reaching a plateau potential after ten to fifteen presynaptic spikes, sometimes increasing again in amplitude after twenty to twenty-five spikes. This plateau was typically similar in absolute voltage to the peak of the single-spike IPSP for a relatively wide range of firing rates (100–250 Hz). Following up to ten to fifteen presynaptic spikes (150–200 Hz) the decay of the last IPSP in the train was similar to or even faster than that for single spike IPSPs. However, when > 20 presynaptic spikes were elicited (220–250 Hz, $n = 4$) a slower decay was also observed (see Figs 7 and 11, $n = 4$ of 4 IPSPs tested in this way). The amplitude and decay rate of this later event appeared to depend on the number of spikes elicited.

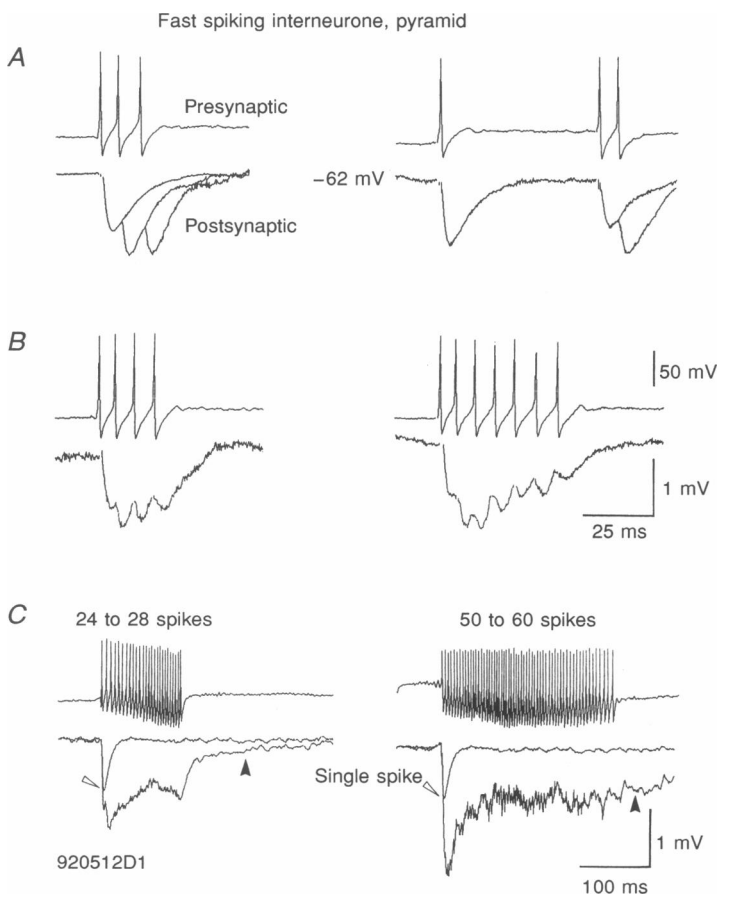

Figure 11. Averaged IPSPs elicited by a classical fast spiking interneurone in a simultaneously recorded pyramidal cell (920512D1)

All IPSPs recorded at −62 mV. Averages include between 100 and 200 sweeps for *A* and between 5 and 20 sweeps for *B* and *C*. Voltage scales apply to all traces; time scale in *B* also applies to *A*. *A* shows composite averaged IPSPs comprising postsynaptic responses to single presynaptic spikes, postsynaptic responses to pairs of presynaptic spikes (averages triggered from the rising phase of the 2nd presynaptic spike) and postsynaptic responses to 3-spike trains (triggered from the rising phase of the 3rd presynaptic spike). Pre-spike baselines were matched when these averages were superimposed. *B* shows averages of 4- (left-hand side) and 7-spike IPSPs. Composite averages were triggered from the 1st spikes and the 4th spikes in the trains. *C* shows averaged responses to 24–28 (left-hand side) and 50–60 spike trains (3 point averaged), with averaged responses to single presynaptic spikes superimposed. Filled arrowheads mark the late slow component that follows these longer spike trains.

IPSPs delay spike firing and reset inherent rhythms in pyramidal cells

As described previously in the hippocampus (Miles & Wong, 1984; Miles, 1991; Cobb *et al.* 1995), the IPSP elicited by a single presynaptic interneurone can delay postsynaptic action potentials and entrain inherent rhythms in pyramidal cells. Postsynaptic pyramidal cells were depolarized to firing threshold, either with square-wave current pulses, or DC current. All the larger IPSPs studied ($n = 10$, peak amplitude > 1 mV at −55 mV) delayed spike activation by current pulses. IPSPs with the briefest widths at half-amplitude delayed spikes by 20–30 ms while the longest IPSPs could delay the spike for 50–100 ms. During trains of summing IPSPs, postsynaptic spikes could only be elicited when larger depolarizing pulses were applied and here, spikes only occurred during the decay phase of IPSPs. During DC current injection, pyramidal cells exhibited an oscillating membrane potential and fired spontaneously. As shown in Fig. 13, IPSPs elicited under these conditions were followed by a depolarizing potential that often initiated an action potential. The strongest 'entrainment' was often observed with summing IPSPs and when a spontaneous postsynaptic action potential occurred between 60 and 80 ms before the interneurone spike, so that the IPSP added to and prolonged the spike AHP. Under these conditions, the pyramidal cell fired in a relatively narrow time window after each IPSP, or brief train of IPSPs.

Disynaptic IPSPs

On three occasions when two pyramidal cells were recorded simultaneously, one pyramid elicited a large IPSP in the other (see Fig. 14). These disynaptic IPSPs were similar in several respects to the monosynaptic IPSPs described above. There were, however, important differences. First, these disynaptic IPSPs were rarely activated by a single spike in the presynaptic pyramidal cell (Fig. 14*A*). Two, or in one case, three presynaptic spikes were required (Fig. 14*B*). Second, the latency was longer (> 4 ms) than in monosynaptic connections and variable, even following the 2nd spike of a short interval pair of presynaptic pyramidal spikes. Unlike the monosynaptic IPSPs described above, triggering the average from the rising phase of the IPSP resulted in a faster time to peak than triggering from the 2nd presynaptic action potential, indicating some fluctuation in latency (Fig. 14*D*). Finally, these IPSPs failed in between 10 and 30% of trials, even when large IPSPs could be elicited by pairs of presynaptic spikes (compare IPSP amplitudes in Fig. 14*B* and *D*; see also Miles (1991) for similar observations in CA3).

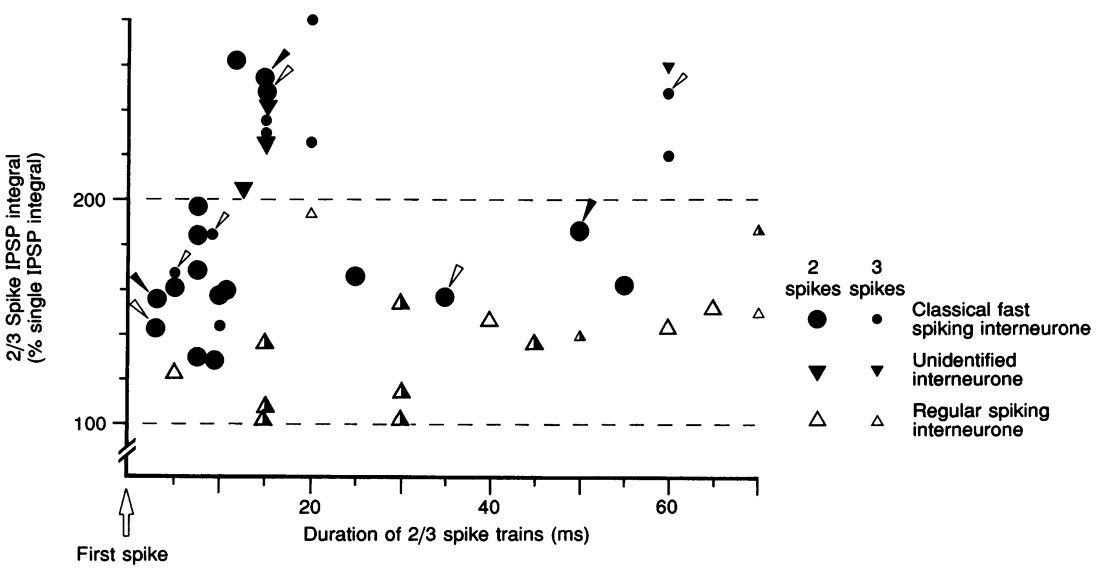

Figure 12. The effects on IPSP integrals of different interspike intervals

The areas under averaged IPSPs elicited by 2-spike (larger symbols) or 3-spike trains (smaller symbols) were integrated and expressed as a percentage of the IPSP elicited by a single spike under the same conditions. If the 2nd spike doubled the total area under the IPSP, the 2-spike point would fall on the 200% line. Second IPSPs that added nothing to the single spike IPSP would fall on the 100% line. Integrals are plotted against the train duration, i.e. the interval between the 1st and 2nd spike (large symbols) or the interval between the 1st and 3rd spike (smaller symbols). Classical fast spiking interneurone IPSPs (data from 9 pairs) are plotted as filled circles. For two of these pairs recorded with a range of interspike intervals, points are marked by open and filled arrowheads, respectively. Unclassified interneurone IPSPs are plotted as filled inverted triangles (2 pairs) and two IPSPs resulting from regular spiking interneurones as open and half-filled triangles, respectively. The IPSPs illustrated by the half-filled triangles were recorded at three different membrane potentials (−50, −53 and −58 mV). At −58 mV the degree of paired pulse depression at 15 and 30 ms was greatest and it was least at −53 mV.

DISCUSSION

Identity of classical fast spiking interneurones?

This paper describes some of the basic properties of IPSPs elicited by classical fast spiking, aspiny interneurones in neocortical pyramidal cells and compares these with IPSPs elicited by other classes of interneurone. Only two of the ten connections made by classical fast spiking interneurones were fully reconstructed histologically after recording the IPSP. In one case the synapses were confirmed at the EM level. These connections, involving three and five boutons (see Figs 6 and 9), resulted in two of the smaller IPSPs recorded (< 0·4 mV at −55 mV). The largest IPSPs recorded (> 2 mV) might therefore have resulted from twelve to twenty boutons. However, to date no recorded connection involving this many synapses has been reconstructed in neocortex. Up to twelve synapses from a single basket cell axon have been reported to innervate a single pyramidal cell in CA1 (Buhl *et al.* 1994*a*) and up to nine in CA3 (Gulyás *et al.* 1993).

In addition to these full pair reconstructions, one other presynaptic classical fast spiking interneurone (postsynaptic partner poorly labelled) and a further four cells with the same electrophysiological characteristics were recovered and are illustrated. Despite strong differences in the shapes of their axonal arbours (see also Kawaguchi, 1995), all the classical fast spiking cells recovered appeared to innervate

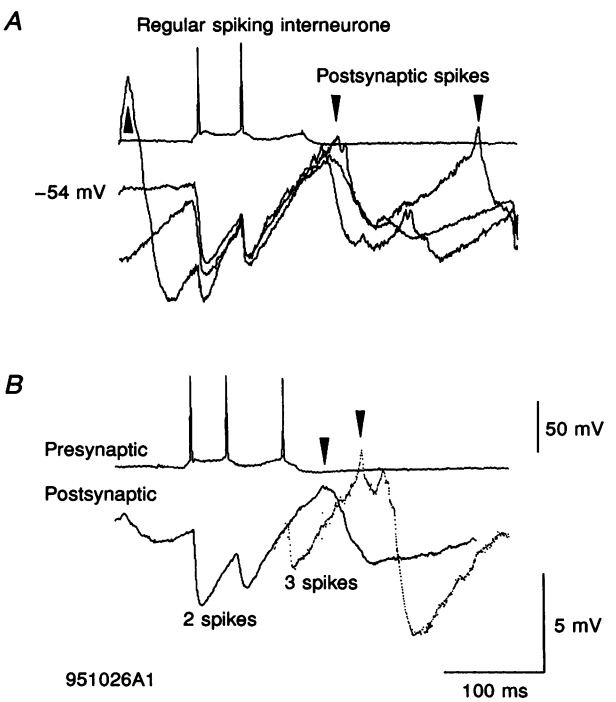

Figure 13. Averaged IPSPs elicited by a regular spiking interneurone in a simultaneously recorded pyramidal cell (951026A1) that was held close to firing threshold by DC current injection (average −54 mV)

Postsynaptic action potentials were severely truncated by the collection programme and when averaged appear only as a positive peak in the voltage trace. The amplitude and sharpness of the peak indicate the consistency of spike latency. Each average consists of at least 20 sweeps. In *A* the averaged IPSPs were elicited by spike pairs. Averages were triggered by the 2nd presynaptic spike. The three averages result from three data subsets in which records were selected according to the events in the postsynaptic cell that preceded the presynaptic spike. In one data set, the membrane potential was relatively steady for 100 ms before the presynaptic spike. This data set resulted in the least consistent post-IPSP spike firing. In another set (see arrowhead) a spontaneous postsynaptic spike preceded the presynaptic spike by 63–76 ms. It was in this set that postsynaptic spikes most consistently followed the IPSP (resulting in the largest positive peaks), two postsynaptic spikes occurring at fairly constant latencies in the majority of sweeps (see inverted arrowheads). The interval between these two peaks gives an indication of the peak spontaneous firing rate of the postsynaptic pyramid and the delay introduced by the IPSPs. In the 3rd, the postsynaptic spike preceded the presynaptic spike by > 150 and < 200 ms. In *B* the effects of 2- and 3-spike IPSPs are compared. All the sweeps illustrated in *A* were averaged together (continuous trace). An average of 3-spike IPSPs from the same data set was then triggered from the rising phase of the 3rd spike (dotted trace). The addition of a 3rd-spike IPSP delays the spike further and triggers more consistent post-IPSP firing. This is evident in the shape of the averaged post-spike AHP, which is less smoothed than in 2-spike IPSP averages. Note, however, that the additional delay introduced by the 3rd IPSP is less than the interval between the 2nd and 3rd spikes.

somata and/or dendritic shafts of spiny cells preferentially (some of which were identified as pyramidal cells). Although the axon of only one of seven cells studied at the EM level (Table 1) appeared preferentially to innervate somata (14 of 19 boutons studied), as might be expected of a classical basket cell, in cat neocortex the target profile of the majority of basket cells included substantially less than 50% somatic contacts (e.g. Jones & Hendry, 1984). The widely different spatial extent and shapes of the axonal arbours suggests that the regions of cortex under the direct inhibitory control of these cells varies from discrete regions of a single layer to more extensive regions of several layers.

In the hippocampus, interneurones can be more readily classified as, for example, basket or bistratified cells because of the more ordered laminar structure. In neocortex, somata, apical and basal dendrites and axons of pyramidal cells are found in almost all layers and the shape and location of the axonal arbours give few clues as to the target specificity. Confirmation of the proximity of boutons to the postsynaptic soma often requires full reconstruction of postsynaptic targets. It may therefore be too early to attempt to classify these neurones further. The possibility exists that some of the recorded IPSPs resulted from chandelier inputs, but to date, no such interneurone has been fully recovered and only one chandelier-type axon has been observed in this study following a recording of a fast spiking neocortical neurone. It appears that in rat neocortex, classical fast spiking interneurones contact one in four or five of their close pyramidal cell neighbours with between one and possibly up to twenty often proximally located synaptic boutons. The targets of nine randomly selected boutons of a presumed regular spiking interneurone axon were similar, i.e. four somata, five dendrites.

Different types of $GABA_A$ receptor-mediated IPSPs?

Although they varied widely in amplitude from pair to pair, the IPSPs generated by classical fast spiking interneurones were consistently fast in time course (width at half-amplitude, $14{\cdot}72 \pm 3{\cdot}83$ ms) and extrapolated reversal potentials were also consistent with mediation by $GABA_A$ receptors. IPSPs elicited by fast spiking interneurones with shallower spike AHPs and accommodating spike firing were similar in their properties (half-width, $16{\cdot}8 \pm 7{\cdot}06$ ms).

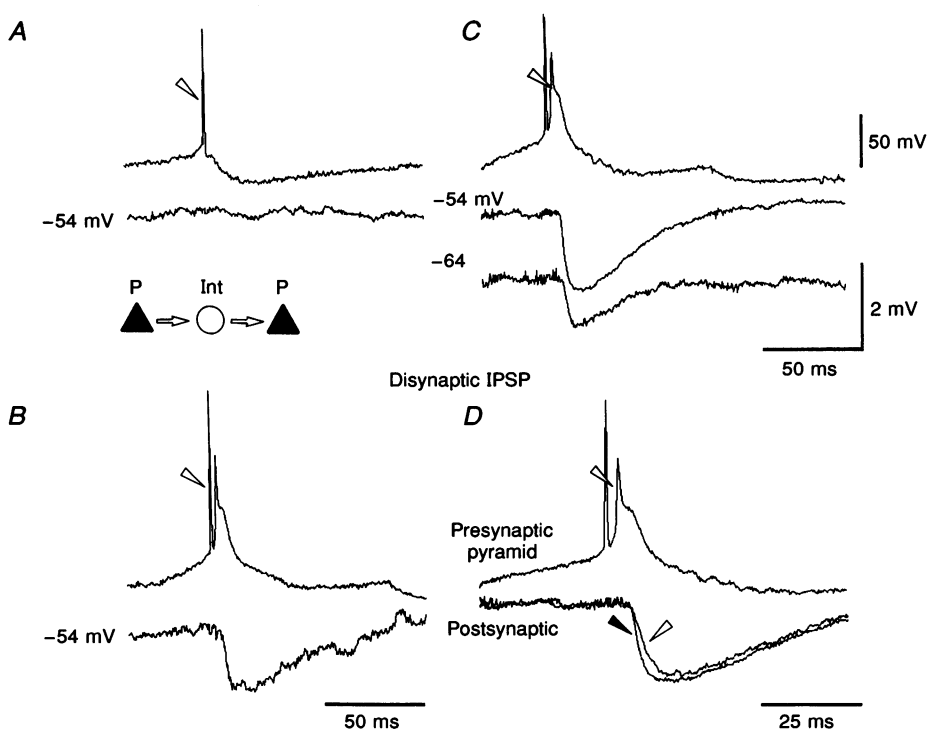

Figure 14. Disynaptic IPSPs elicited in one pyramidal cell by short interval spike pairs in another pyramidal cell (scheme below *A* indicates probable circuit)

Averages consist of between 100 and 200 sweeps. *A* shows averaged postsynaptic responses to single presynaptic spikes. IPSPs were only very rarely elicited by single spikes. *B*, *C* and *D* show averaged responses to pairs of pyramidal spikes. In *B* all 2-spike sweeps are included and the average was triggered by the 1st presynaptic spike (see arrowhead). In approximately 25% of sweeps there was no apparent postsynaptic response. In *C* and *D*, only those sweeps in which an IPSP was apparent were included in the averages (−54 mV traces include the same sweeps in *C* and *D*). In *C* averages were triggered by the 2nd presynaptic spike and IPSPs recorded at two different membrane potentials are shown. In *D*, 2 averages are shown on an expanded time base. One (see open arrowhead) was triggered by the 2nd presynaptic spike; the other (filled arrowhead) was triggered by the rising phase of the IPSP.

Regular spiking interneurones with electrophysiological characteristics similar to pyramidal cells elicited intermediate duration IPSPs (half-width, 27·3 ± 3·68 ms) and unclassified, or slow interneurones elicited the broadest IPSPs (half-width, 56·29 ± 23·44 ms). Thus the IPSPs elicited by two other broad groups of interneurones were slower in time course. However, these slower IPSPs exhibited similarly short latencies and similar amplitudes and appeared to be no less sensitive to current injected at the postsynaptic soma. Previous studies of single axon excitatory postsynaptic potentials (EPSPs) in neocortical pyramidal cells have demonstrated correlations between synapse location, EPSP time course and sensitivity to current injected at the soma (Thomson *et al.* 1993*a*; Deuchars, West & Thomson, 1994). Distally located inputs resulted in slower EPSPs that were almost insensitive to current injected at the soma. In this and a previous study in hippocampus, however (Miles, 1990), no correlation was found between IPSP time course and amplitude. The present data would therefore suggest that most of the synapses contributing to the recorded IPSPs were relatively proximally located, as indicated by the anatomical reconstructions, except for those elicited by burst-firing interneurones.

There is no indication from the present data therefore that either of these slower IPSPs was generated at a significantly more distal dendritic location, or that it was mediated primarily by $GABA_B$ receptors. Fast IPSPs elicited by spiny, burst-firing interneurones may in contrast involve more distal contacts, since in this and a previous study (Deuchars & Thomson, 1995*a*), IPSPs elicited by spiny interneurones were only recorded when the postsynaptic electrode was located in a pyramidal cell dendrite. Spiny interneurone IPSPs were insensitive to a $GABA_B$ antagonist and reversed at membrane potentials less negative than −80 mV. It may be reasonable to propose therefore that at least four broad classes of interneurones activate $GABA_A$ receptor-mediated IPSPs in pyramidal cells, three at relatively proximal sites. Moreover the different classes of interneurone may activate $GABA_A$ receptors with different properties. Recent cloning and expression studies have indicated that a wide diversity of putative $GABA_A$ receptor/channels could exist in the central nervous system (Lüddens *et al.* 1995; Sieghart, 1995). It remains to be determined whether the properties of single axon IPSPs can be correlated with $GABA_A$ receptor subunit expression.

One concern was that the slower time course of some IPSPs might have resulted from the continued presence of the pentobarbitone used as the anaesthetic in later experiments. However, the effects of similar concentrations of pentobarbitone reverse during 1–2 h wash (authors' unpublished data) and all recordings reported were made after more than 4 h incubation. There was no correlation between the 'wash' time and the IPSP time course in the present study and similarly fast IPSPs were recorded in early and later experiments (i.e. without and with pentobarbitone anaesthesia). In addition, powerful effects on neocortical IPSPs have been observed following additional pentobarbitone administration under the same experimental conditions (authors' unpublished data).

IPSP frequency following

Since fast IPSPs summed at interspike intervals < 20–40 ms, it was not possible to obtain an accurate measurement of 2nd IPSP amplitude without subtraction. To study the effects of different interspike intervals therefore, summed IPSPs were integrated and expressed as a percentage of the area under IPSPs elicited by single presynaptic spikes. Measured in this way IPSPs displayed paired pulse depression at interspike intervals < 10 and between 20 and 60 ms. Between 10 and 20 ms some degree of paired pulse facilitation was observed. Third spikes in bursts < 20 ms in duration elicited a summed IPSP with a greater peak amplitude than spike pairs occurring within the same time window, but added relatively little to the integrated response. In addition, while higher firing rates increased the peak amplitude of a summed IPSP, they had little effect on the plateau potential achieved during a train. For relatively brief spike trains therefore there may be an optimal interspike interval. The mechanisms underlying these paired pulse effects are likely to be complex, involving both pre- and postsynaptic mechanisms. That non-linear summation of IPSPs may contribute was indicated when paired pulse depression was reduced by depolarizing the postsynaptic membrane (half-filled triangles, Fig. 12). This indicates that while the voltage response may indicate profound paired pulse depression, the conductance underlying the second or subsequent IPSPs might be less affected.

A late slow hyperpolarizing event follows the summed fast IPSP

The extremely high firing frequencies that classical fast spiking interneurones can maintain for long periods may not greatly enhance the summed, fast, $GABA_A$ receptor-mediated event, but may have an additional effect. In four IPSPs studied with long presynaptic spike trains, a slowly decaying hyperpolarizing event was observed to follow the summed fast IPSP. This was not apparent unless > 20 spikes occurred at > 100 Hz, but could be repeatedly activated at one per 3–5 s. It could not be initiated by current injection into the postsynaptic soma. Its slow onset (> 50 ms after the start of the spike train) and decay (> 200 ms) might indicate that it results from activation or depression of ion channels that are not directly ligand gated.

$GABA_B$ receptor-mediated IPSPs are slower in onset and decay than $GABA_A$ receptor-mediated IPSPs (Connors *et al.* 1988). They may also require stronger presynaptic activation, since spontaneous 'slow' $GABA_B$ IPSPs were only observed in the dentate gyrus in the presence of K^+ channel blockers applied to enhance spike-triggered transmitter release (e.g. Otis, De Koninck & Mody, 1993). Similarly, GABA uptake blockers can enhance or reveal previously unmeasurable stimulus-elicited slow IPSPs

(Thompson & Gähwiler, 1992). It is almost impossible, in the absence of dual recordings, to assess the number of normal presynaptic spikes that might be required to initiate a 'slow' $GABA_B$ IPSP. Many of the protocols used previously might have activated bursts of presynaptic spikes simultaneously in several presynaptic interneurones. Onset latencies for stimulus-elicited slow IPSPs are not typically as long as those reported here (e.g. Crunelli, Haby, Jassik-Gerschenfeld, Leresche & Pirchio, 1987; Connors *et al.* 1988), but in the present study, only one interneurone was directly activated. On the other hand, a number of studies (Williams & Lacaille, 1992; Sugita *et al.* 1992; Otis & Mody, 1992; Samulack & Lacaille, 1993; Otis *et al.* 1993; Kang *et al.* 1994; Benardo, 1994) have indicated that $GABA_A$ and $GABA_B$ receptor-mediated IPSPs originate from different presynaptic neurones in both neocortex and hippocampus. The voltage dependence and pharmacology of the late slow event reported here remain to be studied. It is therefore unclear at present whether classical fast spiking interneurones can activate $GABA_B$ receptors if they only fire rapidly and for long enough, or whether another transmitter is released from these neurones. To date, however, there are no reports of colocalization of parvalbumin and any known neuroactive peptide in neocortical interneurones.

Fast IPSPs in the local circuit

In two previous studies, the EPSPs elicited by pyramidal cells in two classes of neocortical interneurone were found to display strong paired pulse facilitation (Thomson, Deuchars & West, 1993*b*; Thomson & Deuchars, 1994; Thomson *et al.* 1995). The EPSPs typically showed large fluctuations in amplitude (see also Fig. 7) and a high probability of transmission failure with single presynaptic spikes, but increased in amplitude with spike pairs < 50 ms in duration. The 3rd, 4th and 5th spikes often elicited increasingly large events over a wider range of interspike intervals. The disynaptic IPSPs reported here are consistent with this previous finding and those of Miles & Wong (1984) and Miles (1991). In these disynaptic pairs, single pyramidal spikes elicited almost no response in the other pyramidal cell, but short interval spike pairs (and in one case spike triplets) elicited a large disynaptic IPSP. Clearly, the firing of a single pyramidal neurone is sufficient to fire an interneurone, provided the pyramid fires some brief pairs, or bursts of action potentials.

A single pyramidal cell might therefore be able drive a fast spiking interneurone close to an optimal frequency for eliciting summing fast IPSPs, but the late slow event appears to require somewhat higher firing rates. EPSPs in interneurones have a rapid time course and if they reach firing threshold, initiate single spikes at nearly invariant latencies. The rapid and deep interneurone AHP prevents activation of additional spikes during that EPSP, but facilitates reactivation with a second EPSP, or during a maintained depolarization. To maintain firing rates of > 150 Hz, higher than pyramidal cells typically maintain, it is likely that summed excitatory inputs from several sources would be required.

As previously described in hippocampus (Cobb *et al.* 1995) a single axon IPSP can 'entrain' the membrane oscillations and firing of a pyramidal cell. Similar effects were observed in the present study. Moreover, the disynaptic data presented here would also suggest that under appropriate conditions, the firing of one pyramidal cell could, via one or more interneurones, entrain the activity of other pyramidal cells. The different firing characteristics of the several classes of interneurones and the different durations of the IPSPs that they elicit may indicate that they perform different roles in the circuit.

Benardo, L. S. (1994). Separate activation of fast and slow inhibitory postsynaptic potentials in rat neocortex *in vitro*. *Journal of Physiology* **476**, 203–215.

Buhl, E. H., Cobb, S. R., Halasy, K. & Somogyi, P. (1995). Properties of unitary IPSPs evoked by anatomically identified basket cells in the rat hippocampus. *European Journal of Neuroscience* **7**, 1989–2004.

Buhl, E. H., Halasy, K. & Somogyi, P. (1994*a*). Diverse sources of hippocampal unitary inhibitory postsynaptic potentials and the number of synaptic release sites. *Nature* **368**, 823–828.

Buhl, E. H., Han, Z.-S., Lörinczi, Z., Stezhka, V. V., Karnup, S. V. & Somogyi, P. (1994*b*). Physiological properties of anatomically identified axo-axonic cells in the rat hippocampus. *Journal of Neurophysiology* **71**, 1289–1307.

Buhl, E. H., Szilágyi, T., Halasy, K. & Somogyi, P. (1996). Physiological properties of anatomically identified basket and bistratified cells in the CA1 area of the rat hippocampus *in vitro*. *Hippocampus* **6**, 294–305.

Celio, M. R. (1986). Parvalbumin in most γ-aminobutyric acid-containing neurons in the rat cerebral cortex. *Science* **231**, 995–996.

Cobb, S. R., Buhl, E. H., Halasy, K., Paulsen, O. & Somogyi, P. (1995). Synchronization of neuronal activity in hippocampus by individual GABAergic interneurons. *Nature* **378**, 75–78.

Condé, F., Lund, J. S., Jacobowitz, D. M., Baimbridge, K. G. & Lewis, D. A. (1994). Local circuit neurons immunoreactive for calretinin, calbindin D-28k or parvalbumin in monkey prefrontal cortex: Distribution and morphology. *Journal of Comparative Neurology* **341**, 95–116.

Connors, B. W., Malenka, R. C. & Silva, L. R. (1988). Two inhibitory postsynaptic potentials and $GABA_A$ and $GABA_B$ receptor-mediated responses in neocortex of rat and cat. *Journal of Physiology* **406**, 443–468.

Crunelli, V., Haby, M., Jassik-Gerschenfeld, D., Leresche, N. & Pirchio, M. C. (1987). Cl^- and K^+ dependent inhibitory postsynaptic potentials evoked by interneurones of the rat lateral geniculate nucleus. *Journal of Physiology* **399**, 153–176.

DeFelipe, J., Hendry, S. H. & Jones, E. G. (1989). Synapses of double bouquet cells in monkey cerebral cortex visualized by calbindin immunoreactivity. *Brain Research* **503**, 49–54.

Del Rio, M. R. & DeFelipe, J. (1994). A study of SMI 32-stained pyramidal cells, parvalbumin-immunoreactive chandelier cells, and presumptive thalamocortical axons in the human temporal neocortex. *Journal of Comparative Neurology* **342**, 389–408.

Deuchars, J. & Thomson, A. M. (1995*a*). Single axon fast inhibitory postsynaptic potentials elicited by a sparsely spiny interneuron in rat neocortex. *Neuroscience* **65**, 935–942.

Deuchars, J. & Thomson, A. M. (1995*b*). Innervation of burst firing spiny interneurons by pyramidal cells in deep layers of rat somatomotor cortex: Paired intracellular recordings with biocytin filling. *Neuroscience* **69**, 739–755.

Deuchars, J., West, D. C. & Thomson, A. M. (1994). Relationships between morphology and physiology of pyramid–pyramid single axon connections in rat neocortex *in vitro*. *Journal of Physiology* **478**, 423–435.

Gulyás, A. I., Miles, R., Hájos, N. & Freund, T. F. (1993). Precision and variability in postsynaptic target selection of inhibitory cells in the hippocampal CA3 region. *European Journal of Neuroscience* **5**, 1729–1751.

Gulyás, A. I., Toth, K., Danos, P. & Freund, T. F. (1991). Subpopulations of GABAergic neurons containing parvalbumin, calbindin D28k, and cholecystokinin in the rat hippocampus. *Journal of Comparative Neurology* **312**, 371–378.

Han, Z.-S., Buhl, E. H., Lörinczi, Z. & Somogyi, P. (1993). A high degree of spatial selectivity in the axonal and dendritic domains of physiologically identified local-circuit neurons in the dentate gyrus of the rat hippocampus. *European Journal of Neuroscience* **5**, 395–410.

Jones, E. G. & Hendry, S. H. C. (1984). Basket cells. In *Cerebral Cortex*, vol. 1, *Cellular Components of the Cerebral Cortex*, ed. Peters, A. & Jones, E. G., pp. 309–336. Plenum Press, New York.

Kang, Y., Kaneko, T., Ohishi, H., Endo, K. & Araki, T. (1994). Spatiotemporally differential inhibition of pyramidal cells in the cat motor cortex. *Journal of Neurophysiology* **71**, 280–293.

Kawaguchi, Y. (1995). Physiological subgroups of non-pyramidal cells with specific morphological characteristics in layers II/III of rat frontal cortex. *Journal of Neuroscience* **15**, 2638–2655.

Kawaguchi, Y. & Hama, K. (1988). Physiological heterogeneity of nonpyramidal cells in rat hippocampal CA1-region. *Experimental Brain Research* **72**, 494–502.

Kawaguchi, Y. & Kubota, Y. (1993). Correlation of physiological subgroupings of nonpyramidal cells with parvalbumin- and calbindinD28k-immunoreactive neurons in layer V of rat frontal cortex. *Journal of Neurophysiology* **70**, 387–396.

Kisvárday, Z. F. (1992). GABAergic networks of basket cells in the visual cortex. *Progress in Brain Research* **90**, 385–405.

Kisvárday, Z. F., Beaulieu, C. & Eysel, U. T. (1993). Network of GABAergic large basket cells in cat visual cortex (area 18): Implication for lateral disinhibition. *Journal of Comparative Neurology* **327**, 398–415.

Lacaille, J.-C. & Schwartzkroin, P. A. (1988). Stratum-lacunosum-molleculare interneurons of hippocampal CA1 region. II Intrasomatic and intradendritic recordings of local circuit synaptic interactions. *Journal of Neuroscience* **8**, 1400–1410.

Li, X.-G., Somogyi, P., Tepper, J. M. & Buzsáki, G. (1992). Axonal and dendritic arborization of an intracellularly labelled chandelier cell in the CA1 region of the rat hippocampus. *Experimental Brain Research* **90**, 519–525.

Lüddens, H., Korpi, E. R. & Seeburg, P. H. (1995). $GABA_A$/benzodiazepine receptor heterogeneity: Neurophysiological implications. *Neuropharmacology* **34**, 245–254.

Miles, R. (1990). Variation in strength of inhibitory synapses in the CA3 region of guinea-pig hippocampus *in vitro*. *Journal of Physiology* **431**, 659–676.

Miles, R. (1991). Tetanic stimuli induce a short-term enhancement of recurrent inhibition in the CA3 region of guinea-pig hippocampus *in vitro*. *Journal of Physiology* **443**, 669–682.

Miles, R. & Wong, R. K. S. (1984). Unitary inhibitory synaptic potentials in the guinea-pig hippocampus *in vitro*. *Journal of Physiology* **356**, 97–113.

Otis, T. S., De Koninck, Y. & Mody, I. (1993). Characterization of synaptically elicited $GABA_B$ responses using patch-clamp recordings in rat hippocampal slices. *Journal of Physiology* **463**, 391–407.

Otis, T. S. & Mody, I. (1992). Differential activation of $GABA_A$ and $GABA_B$ receptors by spontaneously released transmitter. *Journal of Neurophysiology* **67**, 227–234.

Samulack, D. D. & Lacaille, J.-C. (1993). Hyperpolarizing synaptic potentials evoked in CA1 pyramidal cells by glutamate stimulation of interneurons from the oriens/alveus border of rat hippocampal slices. II. Sensitivity to GABA antagonists. *Hippocampus* **3**, 345–358.

Sieghart, W. (1995). Structure and pharmacology of γ-aminobutyric $acid_A$ receptor subtypes. *Pharmacological Reviews* **47**, 181–234.

Sik, A., Penttonen, M., Ylinen, A. & Buzsáki, G. (1995). Hippocampal CA1 interneurons: An *in vivo* intracellular labelling study. *Journal of Neuroscience* **15**, 6651–6665.

Somogyi, P. (1977). A specific axo-axonal neuron in the visual cortex of the rat. *Brain Research* **136**, 345–350.

Sugita, S., Johnson, S. W. & North, R. A. (1992). Synaptic inputs to $GABA_A$ and $GABA_B$ receptors originate from discrete afferent neurons. *Neuroscience Letters* **134**, 207–211.

Thompson, S. M. & Gähwiler, B. H. (1992). Effects of the GABA uptake inhibitor tiagabine on inhibitory synaptic potentials in rat hippocampal slice cultures. *Journal of Neurophysiology* **67**, 1698–1701.

Thomson, A. M. & Deuchars, J. (1994). Temporal and spatial properties of local circuits in neocortex. *Trends in Neurosciences* **17**, 119–126.

Thomson, A. M., Deuchars, J. & West, D. C. (1993*a*). Large, deep layer pyramid–pyramid single axon EPSPs in slices of rat motor cortex display paired pulse and frequency-dependent depression, mediated presynaptically and self-facilitation, mediated postsynaptically. *Journal of Neurophysiology* **70**, 2354–2369.

Thomson, A. M., Deuchars, J. & West, D. C. (1993*b*). Single axon excitatory postsynaptic potentials in neocortical interneurons exhibit pronounced paired pulse facilitation. *Neuroscience* **54**, 347–360.

Thomson, A. M., West, D. C. & Deuchars, J. (1995). Properties of single axon excitatory postsynaptic potentials elicited in spiny interneurons by action potentials in pyramidal neurons in slices of rat neocortex. *Neuroscience* **69**, 727–738.

Williams, S. & Lacaille, J.-C. (1992). $GABA_B$ receptor-mediated inhibitory postsynaptic potentials evoked by electrical stimulation and by glutamate stimulation of interneurons in stratum lacunosum-moleculare in hippocampal CA1 pyramidal cells *in vitro*. *Synapse* **11**, 249–258.

Acknowledgements

We would like to thank the Medical Research Council, Sandoz Pharma (Basel) and The Wellcome Trust for financial support.

Author's email address

A. M. Thomson: alext@rfhsm.ac.uk

Received 2 April 1996; accepted 21 June 1996.